A Network Camera with a Nose

Applications and Evalutation of Low-cost Air Sensors

Rasmus Björklund Eric Kuan

September 25, 2018

LUND
UNIVERSITY

Master´s Thesis in

Electrical Measurements

Faculty of Engineering LTH
Department of Biomedical Engineering

Supervisors: Johan Nilsson (LTH), Lars Andersson and Freddie Olsson
Examiner: Lars Wallman

Abstract

Some network cameras have already several other sensors besides the image sensor to extend the capabilities of the camera. It is then only natural to think what can be achieved when air sensors are added into the mix. In this master thesis the applications of air sensors coupled together with network cameras have been investigated. Considering the network infrastructure is already in place, having camera units collecting air quality data is certainly attractive in cities where pollution is a problem. Not only will it help localise the source, it will also aid urban planning. Of course, this is only one of the many application areas of air sensors. Having accurate data is also important as the price of air sensors usually have a relation with their accuracy.

Two prototypes for an low-cost NO_2 electrochemical sensor, Alphasense NO2-B43F, were built that can be connected to a I/O-interface of a network camera for data transmission and power. Another low-cost sensor, the Alphasense OPC-N2, was evaluated, as measurement of particles are interesting. The evaluation was based on comparison with the more expensive counterparts of the low-cost sensor. Climate test were performed for the Alphasense NO2-B43F.

It was concluded that these low-cost sensors have many uncertainties and require various tests, such as long term tests and precision tests. From the performed tests and comparison, the Alphasense NO2-B43F has shown to correlate well enough with the reference measurements to have the potential to supplement the reference with local measurements. The transmission of data and power through a network camera has been successful with the prototype.

Acknowledgements

We want to give a special thanks to our supervisors Lars Andersson and Freddie Olsson. They have helped us a lot with their deep knowledge in electronics and introduced us to a lot of new concepts. Their superb feedback has also been very valuable for the project.

We also want to thank Johan Nilsson, our supervisor at LTH. He has been a good discussion partner and always came with new input and perspectives regarding measurement electronics. When we feel like we have hit a dead end, a meeting with Johan had always resulted with a solution and new energy.

At last we want to thank Mårten Spanne and Malin Alsved for taking their time to help us out with the sensor evaluation and sharing their knowledge about environmental science. When we started this thesis, we did not have any knowledge about air quality monitoring, but they have been patient and given us an insight in the subject. Doing these measurements is complex and there are a lot of aspects to consider. It is truly admirable to see people like them managing it.

Contributions

Many parts of the project were done together by the two members of the project. These parts are in the beginning phase of the project, such as identifying the applications of air sensors, contacting vital persons with knowledge of air quality monitoring and screening through all the available routes. Once sensors and applications were decided the work split naturally. Rasmus Björklund worked on the communication link between the microcontroller and the camera and focused on getting a working measurement set up with the PM-sensor, OPC-N2. The hardware required for the electrochemical sensor, NO2-B43F, was handed over to the other member, Eric Kuan, which resulted in a custom designed PCB that acted as a data acquisition card for the NO2-B43F. The evaluation of the OPC-N2 and regression analysis were mainly done by Rasmus, while the NO2-B43F and its peculiarities, such as the cross sensitivity, were evaluated by Eric.

Contents

Abbreviations

ADC Analog-to-Digital Converter. 33

AQM Air Quality Monitoring. 15

CL Chemiluminescence. 20

CO Carbon Monoxide. 15

DOAS Differential Optical Absorption Spectroscopy. 19

EPA Environmental Protection Agency. 15

EVM Evaluation Module. 35

ISB Individual Sensor Board. 32

LDO Low Dropout. 34

MCU Micro Controller Unit. 30

MOS Metal Oxide Semiconductor. 17

NO_2 Nitrogen Dioxide. 15

NO_x Nitrogen Oxides. 20

O_3 Ground-level Ozone. 15

OPC Optical Partical Counter. 21

PCB Printed Circuit Board. 29

PM Particulate Matter. 15

PTFE Polytetrafluoroethylene. 37

1 Introduction

The master thesis was supervised by the Biomedical Engineering department of Lund University. A camera relies on the image sensor to detect and identify objects. This can be limiting of what the camera can detect but can be mitigated by adding other sensors. For example, adding a microphone allows the camera unit to hear the surroundings and detect danger outside the visual field or when it is too dark for the image sensor to capture light.

Some network cameras have already different sensors to help the camera to monitor the environment. One field of sensors yet to be explored was air sensors to provide additional functionality for network cameras. Since the camera is already online and the network infrastructure already exists, integrating an air sensor into the unit and collecting the data is convenient. Adding more sensors has its disadvantages such as cost and increased complexity of the unit.

1.1 Objectives

The main objective of this thesis is to investigate what can be done when a network camera gains the ability to detect specific components in the air. To support the investigation three more specific objectives were set and as these are met the investigation can be concluded.

- One of the biggest interest in adding an air sensor with the camera is what additional application it can be used in. There are many different components in the air, which are the most interesting to measure? Who will be interested in a camera with these capabilities? Besides measuring the components of the air, can this information be extrapolated to gain additional benefits in other aspects of the camera?

- Many technologies exists with a very wide range of cost and size. The focus will be on technologies with a small footprint and that are cost-effective. This will allow easier integration in a camera or a portable accessory box for a camera. How these units perform compared to more expensive devices will be investigated.

- The development of sensor technologies is always moving forward, especially when small, interconnected sensing devices are rising in popularity. The current technologies can be developed further and allow the more advanced technologies to cut down in price and size or the simpler technologies to mitigate its flaws. There are other aspects than just the development of air sensor technologies. Methods of combining other sensors and data manipulation can also be the solution. What can be expected in the future of low-cost air sensor applications?

2 Methodology

This project will be a mixture between product development and a study of sensor technology. The structure of our development is based on the following key steps:

- Preliminary study
- Development of the prototype
- Evaluation of the prototype
- Improvements

Many different technologies exist to analyse the components in the air and the applications of air sensors are large. A preliminary study was done to determine what application of low-cost air sensor can be useful together with network cameras. Exchanges with people in the field and own research allows further insights of what valuable information air sensors could provide and based on that information the applications of air sensors were determined. Once the application was determined requirements were specified to find a suitable sensor for the application. With the application and the sensor determined, development of a prototype was the next step. Getting data from the chosen sensors as early as possible was prioritised. Early evaluation makes it possible to discover unforeseen flaws and make improvements gradually. As this thesis partly relies on external expertise, having a good time margin makes it easier to plan meetings and borrow instruments.

3 Preliminary study

The aim with the thesis is to investigate how an air sensor can create new areas of use for network cameras.

3.1 Customer needs

A market analysis was conducted to gain further insights of the current and near future interests in air sensors. The analysis was done by searching for articles and contacting key persons in different fields of air measurements. In general, Air Quality Monitoring (AQM) has a growing demand. Smart cities, increased awareness of climate change, quality of life are just a few of many reasons of the growth. Another ever-growing interest are devices that can detect safety hazards earlier. As safety continues to be a concern and air sensor technologies are getting cheaper, there is a great interest in inventing new solutions using low-cost air sensors.

3.1.1 Air quality monitoring

Pollution in the air is a big concern in large cities. During times when there is no wind, the polluted air cannot easily disperse; and as sources of pollution are kept in the city, the levels of pollution can grow dangerously high. Air pollution is a health hazard and many respiratory diseases are linked to long exposure to polluted air. The climate also gets affected by polluted air. Acid rain and the thinning of the ozone layer is caused by polluted air. As more data of air pollution are available, the social awareness can be increased and sources of pollution can be traced.

Air quality is a general term used to describe how pollution-free the air is. There are several groups of gases considered as pollutants. According to United States Environmental Protection Agency (EPA), these are the six common air pollutants [1]:

- Carbon Monoxide (CO)
- Nitrogen Dioxide (NO_2)
- Lead (Pb)
- Sulphur Dioxide (SO_2)
- Ground-level Ozone (O_3)
- Particulate Matter (PM)

Mårten Spanne at Malmö Stad Miljöförvaltningen revealed an interest in simple low-cost interconnected sensors in cities. These would ease urban planning and sources of pollutants can be easier to locate. Adam Kristensson, an associate senior

lecturer at Nuclear Physics of Lund University, like Mårten, showed interest regarding building up a sensor network to gather more data regarding PM. The specific data of interest were PM concentration for particles under 2.5 µm and 10 µm, also known as $PM_{2.5}$ and PM_{10}. Size distribution of particles is also considered as valuable data.

The current low-cost outdoor AQM on the market are often not good enough to be considered equivalent instruments by the Swedish national laboratory for quality assurance of measurement devices, Referenslaboratoriet för tätorts-mätningar, at Stockholm University [2] and therefore cannot be officially used to acquire data to compare with national standards. It can however, be an interesting complement to get a better picture of how pollution differ in specific zones.

3.1.2 Security applications

The purpose of an air sensor accessory box connected to a security camera can be to extend the security capabilities of the camera. This would allow the camera to send an alarm when it detects an abnormal level of a component in the air. Three things that could be relevant to measure for human safety were investigated:

- Smoke and fire detection
- Carbon Monoxide (CO)
- Ground-level Ozone (O_3)

CO is critical to detect in vulnerable places with bad ventilation such as mines. CO does not have a smell and high exposure leads to CO-poisoning which in worst case causes death [3]. O_3 can also cause serious health issues even at low concentrations. O_3 exists in free air and can be created from a reaction with O_2 and single oxygen atoms (O). Higher concentrations can be found in industries where it is used in disinfection and priming applications, among other things.

Smoke detectors could also be a beneficial accessory to a security camera. There are studies achieving this functionality using the image sensor of a camera[4], but no products on the market. The market is full of low-cost fire detectors for consumer use and more advanced devices that promises better detection efficiency are being released. One of these products is the Nest protect (Nest Labs, Inc) which uses dual wavelength scattering [5]. Fire detectors connected to an alarm system has to fulfil the EN 54-7:2001 standard [6]. This standard comprises for instance that the unit should be able to operate without power supply for a certain time and that particles larger than $1{,}3 \pm 0.05$ mm are not allowed to enter the measurement chamber.

An aspect to consider with the applications mentioned is the responsibility, since the well-being of people are dependent on the reliability of the devices. This means that the devices must be tested very thoroughly and that the maker can guarantee that they are properly functioning.

Another application of air sensors is presence detection or indoor occupancy in a closed locale. At the time of writing no product have been found utilising PM sensors for this kind of purposes. Research proves that it is possible to detect and estimate indoor occupancy with a tolerance of four people in an office environment [7]. An investigation about correlation between airborne particles and human presence in a room has also been made, however this investigation did not estimate the number of people in the measured area [8].

3.2 Existing technologies

Several different technologies exist to study gases. These technologies differ vastly in terms of performance and in applications. Depending on application, it could have many different methods to achieve the same thing. The differentiating factor then is how well these different methods are performing in different circumstances. There could be cases where only one method exists, because it is well proven, or the costs makes it the only viable candidate. In this section five different gas measurement technologies will be presented, including what the technology could measure and the typical applications.

3.2.1 Metal Oxide Semiconductor

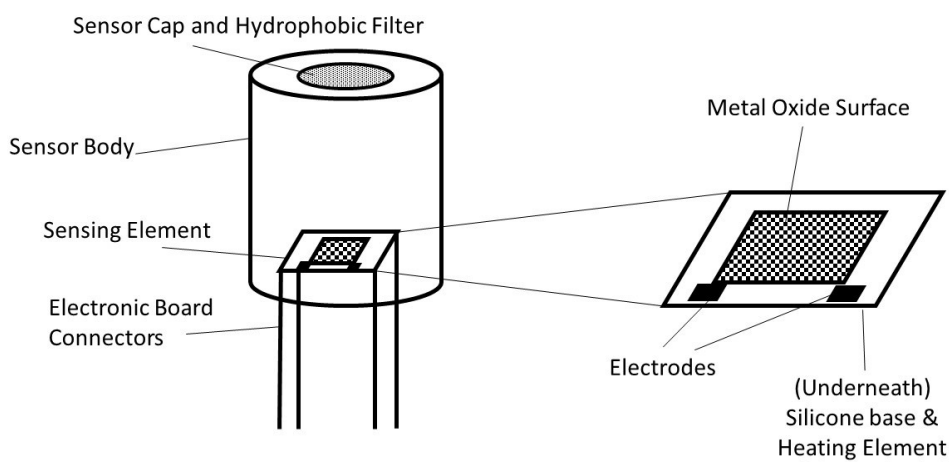

Figure 1: A general description of a MOS gas sensor. The metal oxide surface can be made of different materials depending on the application. A heating element is below the surface to make the surface predictably react to the target gas, and with a reaction a current will flow along the electrodes [9].

Metal Oxide Semiconductor (MOS) gas sensors, Figure 1, are a very flexible sensor-technology used for measuring a specific gas in a gas mixture. The MOS-gas sensors can be made to react to a certain gas by changing the components of metal oxide

layer. The fabrication technologies involved in producing the MOS-gas sensors are similar to other MOS components, making them easy to mass-produce cheaply. MOS-gas sensors have been commonly used as safety devices in industries to detect high levels of gases that could be hazardous. For example, NO_2, O_3, hydrogen sulfide and CO. MOS-sensor are however not commonly used for precise measurements. There are several factors making them unsuitable for such applications. Every MOS-sensor produced has some production variability affecting the conductance of the sensor. Because the conductance is measured to determine the gas concentration, the reproducibility is weak. Cross sensitivity is another noteworthy weakness of MOS-sensors and many other factors such as: temperature, humidity and long-time drifting has a prominent effect, which makes it difficult to compensate [10].

3.2.2 Electrochemical

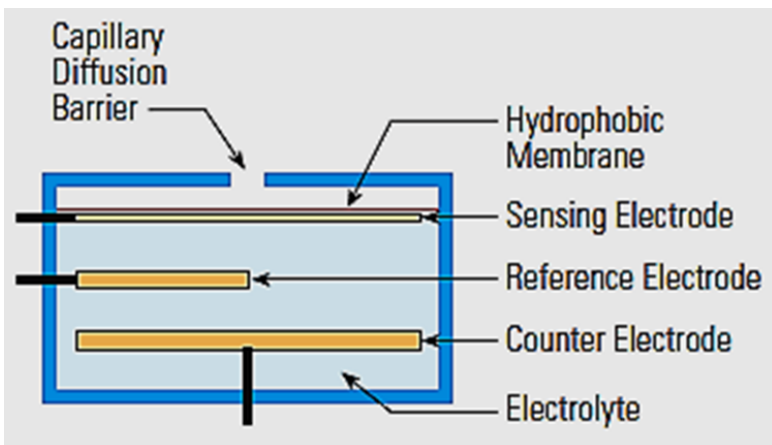

Figure 2: A diagram showing the main components of an electrochemical gas sensor. The sensing electrode will react with the target gas creating excess ions in the electrolyte. In turn the counter electrode will react with the excess ions in the electrolyte [11].

Electrochemical cells are devices made to generate current from chemical reactions or vice versa. Electrochemical gas sensors contain electrochemical cells made to react with the target gas, Figure 2. Like MOS-sensor the electrochemical sensor can be made to measure O_3, CO, NO_2, etc. Unlike MOS-sensors and other technologies, electrochemical sensors have a very low power consumption allowing the electrochemical sensors to be used in portable measuring devices. Electrochemical gas sensors are still limited to indicative measurements and not regulatory measurements. Many of the disadvantages are similar to MOS-sensors, like cross-sensitivity, and besides those the lifespan is limited by how well the electrolyte can keep its properties after drastic changes in humidity.

3.2.3 Absorption Spectroscopy

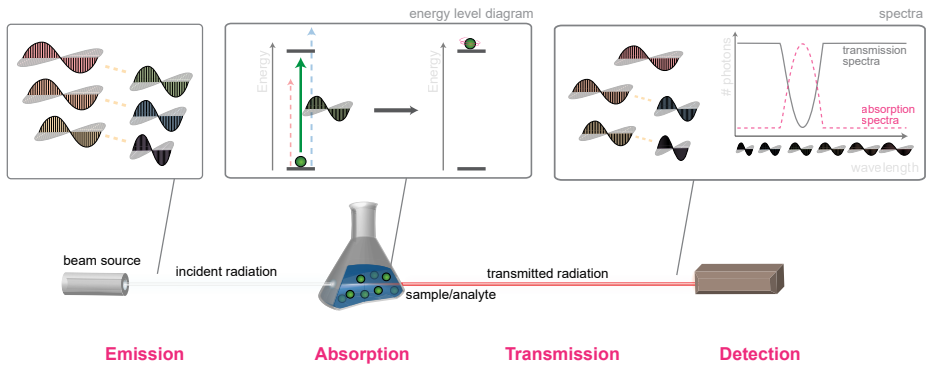

Figure 3: The main steps in absorption spectroscopy. A light is emitted from the light source in the emission step. As the light passes the sample light in different wavelength will be absorbed differently. The transmitted light is received by a detector and from the transmitted light, the absorption spectra of the sample is revealed [12].

Absorption spectroscopy, described in Figure 3, is a versatile measurement method that can be used to measure a wide range of gas concentrations in free air simultaneously. Differential Optical Absorption Spectroscopy (DOAS) is a detection method where the absorption for a longer path is measured. Lund municipality is using this method to collect information about sulphur oxide, NO_2, O_3 and benzene in the urban area [13]. Cavity Attenuated Phase Shift spectroscopy, which is related to Cavity Ringdown Spectroscopy, is also a method employed for this purpose.

Currently, this technology is expensive and measures over a long distance to obtain high sensitivity. Microelectromechanical system units for spectroscopy is upcoming which will push the prices down and make smaller devices available. There are a couple of microelectromechanical system gas sensing devices available. They are however limited to the infrared spectrum, and can only detect gases that absorbs light in the infrared spectrum, such as CO [14]. Gases, such as NO_2, that absorbs light in the ultraviolet spectrum, can not be detected by microelectrochemical system spectroscopy yet.

3.2.4 Chemiluminescence

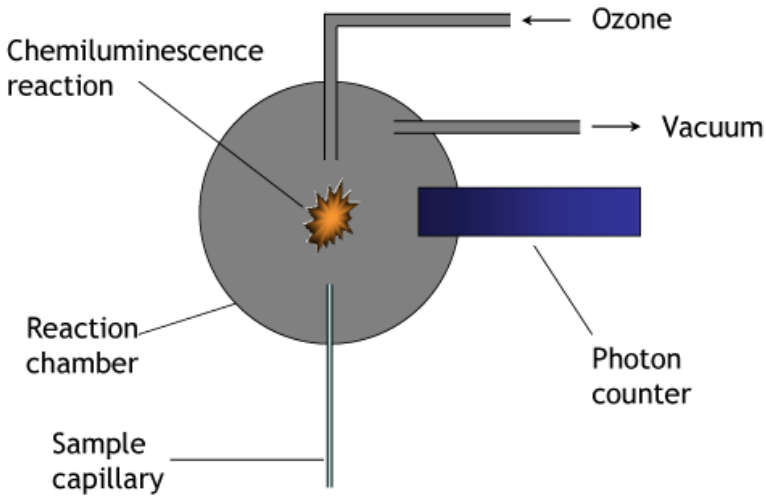

Figure 4: CL is based on the principles of light emission from chemical reactions. In the figure the target gas is NO and the reaction with O_3 creates light [15].

Chemiluminescence (CL) is a technology employed for gas analysis by measuring the emitted light from chemical reactions. This technology is considered as a reference method, [2], for measurements of Nitrogen Oxides (NO_x).It is an indirect method that relies on reducing NO_2. The method can be described in two stages, reduction and CL reaction. Reduction is the first stage of the method. The NO_2 in the sampled gas are reduced to NO. There are several methods of reducing NO_2, using heated molybdenum surfaces, photolysis with xenon lamps or UV emitting diodes. Most of the NO_2 in the sampled gas are reduced, if not all. Once the NO_2 of the sampled gas is reduced to NO it is exposed to O_3 and a gas-phase reaction occurs. The NO_2 formed by the reaction are excited and emits a light. Since the sampled gas contains NO before the reduction the light emitted is both from the sampled NO and the reduced NO_2. Another gas sample is taken and routed to bypass the reduction stage. This gas sample will go through the same gas-phase reaction, but with no NO from the reduced NO_2 the light emitted will only be from the sampled NO molecules. The NO_2 values are then determined by subtracting the value of the first sample with the second sample. By this method the light interference of the sampled NO is eliminated [16][17].

Due to the high cost and size of the instruments it is most commonly seen in wide-area covering measurement stations. Although CL is costly it is still less complex and relatively cheaper than equivalent performing spectroscopic methods [16].

3.2.5 Light scattering

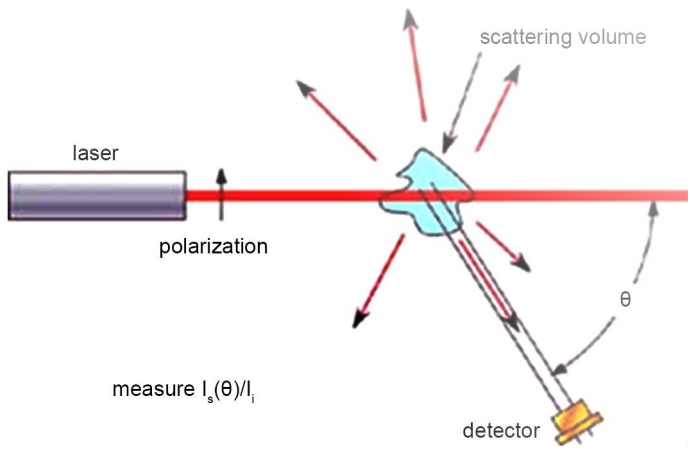

Figure 5: Light scattering uses a light source to emit light. When no particles is in the light's path no light will be detected. As a particle intercept the light, it will bounce off the particle and some of it will reach the detector [18].

Light scattering, Figure 5, is a measurement method that is being used for instance in fire detectors and Optical Partical Counter (OPC). Ionising fire detectors were common back in the days, but with cheaper price tag the light scattering products has become dominating nowadays, especially in the consumer market.

Light scattering is also used to count particles and determine their size. These instruments are called OPC. OPC comes in all kinds of price ranges, everything from compact sensors for home use to certified instruments used for classifying clean rooms. Low-cost sensors often come with some trade-offs in measurement quality to keep the price, size and power consumption down. Software is used to compensate the measurement errors. Since particles comes in many shapes and materials in free air it is difficult to derive a general calibration factor.

3.3 Selection of application area

Two application areas were presented in section 3.1, AQM and security applications. In the first screening, AQM was chosen based on the relevance of what can be accomplished in this thesis. Considering what would generate most interest, AQM in cameras has great potential. Allowing every camera to monitor air quality could provide valuable information for municipalities and with more congested cities in the future and growing health concerns, AQM could bring great value for the society. Another reason for AQM is the emergence of low-cost sensors. The development of new cheaper sensors with different competing technologies makes it interesting to study how they compare to the reference instruments. Analysis could be made to

determine how much these low-cost alternative deviates from the reference. Many network cameras are already in use for traffic surveillance. An opportunity for implementing traffic control is by attaching an AQM accessory to the already installed camera, which is an advantage.

3.4 Air quality measurement considerations

Many pollutants are worth monitoring as mentioned in section 3.1.1. NO_2 and PM measurements was chosen as the two parameters we want to monitor with low-cost sensors. NO_2-measurements with low-cost sensor has been evaluated by others [19][20], but so far, the conclusions have been that the low-cost sensor is not good enough. It is however worth further investigation whether the low-cost sensors are good enough as a complementary measurement device placed around the vicinity of a reference station rather than as a replacement. There is also benefits with more measurement points for NO_2. Most of the generated NO_2 occurs in traffic and with more measurement stations the source can be easier to pinpoint. Considering that NO_2 is a health hazard, knowing where in the city there are high concentrations of NO_2 could help urban planning and traffic control.

Particles have also been shown to be hazardous [21]. With more particle meters placed out around a city more data is available to aid the studies of the hazardous effect of small airborne particles. As many low-cost sensors employ similar methods of measuring PM as some equivalent measurement devices it is becoming more interesting in testing the accuracy of these sensors.

According to United States EPA [22], five tiers of measurements for air measurement devices exist:

- Tier 1: Education and Information
- Tier 2: Hot-spot identification and Characterisation
- Tier 3: Supplementary Network Monitoring
- Tier 4: Personal Exposure Monitoring
- Tier 5: Regulatory Monitoring

These tiers are guidelines rather than pre-defined standards. The goal of this thesis is to aim for Tier 3, which require the deviation to be less than 20 % from a reference instrument. The requirements stated are derived from interviews from different states in the US and does not reflect every states requirement of supplementary network monitoring. The requirements are dependent on the type of pollutant and in the EU the precision can be as low as 50 % and still considerable for Tier 3.

Further insights were revealed by Mårten in what they could consider to be useful. The annual limit for NO_2, in Sweden, is below 20 $\mu g/m^3$, which translates to 10.5 ppb. The national standard also specifies an hourly limit of 60 $\mu g/m^3$, 30 ppb.

Any sensor with higher detection limit will be significantly limited of what data the sensor could provide that could be useful. Better resolution, at around 0.1-0.5 ppb is also preferable. These insights are shared with PM measurements, with the annual limit of 10 µg/m^3 for $PM_{2.5}$ and 15 µg/m^3 for PM_{10}. Specifications on daily limit of $PM_{2.5}$ is 25 µg/m^3 and PM_{10} is 30 µg/m^3 [23].

The cost, size and power requirements of the sensor are important aspects. The cost of the sensor unit must remain below 5000 SEK to be considered viable. As cost is simply not the purchase value of the sensor, the cost of maintaining the sensor must be low as well. The power consumption should be kept low, below 0.3 W if possible, as the I/O-port of the cameras are specified to deliver 25 mA at 12 V . The size of the sensor should be small enough to fit in a box that can be considered portable.

4 Theory

Environmental outdoor AQM has some complexities worth explaining. Under this section the chosen pollutants will be presented along with some general facts about them. The method employed in regulatory monitoring will be explained along with the chosen technology for low-cost sensor as understanding the standard method gives a perspective over what got simplified and compromised to allow the low-cost sensor to measure the same pollutant.

4.1 NO_2 measurement

NO_2 is a reddish-orange-brown gas in room temperature. The colour of the gas is due to the high absorbency in the ultraviolet and visible wavelengths and can reduce visibility in high concentrations. Sources of NO_2 can be natural or human-made. The most prominent human-made source is vehicles with combustion engines and they have the most impact of the concentration levels of NO_2 in urban areas in Sweden. The trend of NO_2 concentrations have been declining but have stagnated in the recent years [24]. The highest annual mean concentration of NO_2 in Malmö, Sweden was at the measurement station in Dalaplan 5B in 2017 with 26 $\mu g/m^3$; this is equivalent to 13 ppb [25]. The European Environment Agency's annual limit value is at 40 $\mu g/m^3$, or 21 ppb. These are very low concentrations and requires very sensitive equipment to detect the NO_2 in the air [26].

Both the CL and spectroscopy method are classified as a reference method [2]. These methods are however very expensive to implement and require a big measurement station to accommodate the instruments and equipment needed. One measurement station, with reference instruments, is estimated to be around 1-2 million SEK and the maintenance costs are around 300 000 SEK each year [27]. Those are the reasons why there are so few measurement stations even on the big cities. The downside of this is the local variation cannot be measured accurately. To capture the local variation more measurement stations needs to be deployed; however, the cost of each additional station must be significantly lower than the cost of the reference station if this would be viable. One way of addressing this problem is by complementing the reference station with sub-stations utilising low-cost sensors.

4.1.1 Electrochemical gas sensors

Low-cost gas sensors, such as electrochemical gas sensors, are interesting candidates to complement the reference measurement stations. Electrochemical gas sensors are a low-cost gas sensor that can be used to measure NO_2. The cost of one sensor unit is around 2000 SEK. The working principle of an electrochemical sensor is based on reduction or oxidation of the target gas. In this case the target gas is NO_2 and the wanted reaction is reduction. The sensor body is a container for the electrolyte. The container has three electrodes: working-, counter- and reference electrode. The

working electrode is in direct contact with the gas diffusion barrier which is exposed to the outside environment. The main purposes of the gas barrier are to direct NO_2 to the working electrode and to protect the electrode. The reaction that occurs in the working electrode is a reduction of the NO_2. The counter electrode is used to balance the reduction at the working electrode with the opposite reaction, oxidation. A current will flow between the two electrodes because of the two simultaneous reactions and the gas concentration is determined by measuring the current, which is related to how strong the reactions are. The purpose of the reference electrode is to keep the voltage of the working electrode constant despite the reactions occurring. By keeping the voltage fixed at a specific potential, good linearity between current and gas concentration can be achieved. This makes it simple to use while maintaining good accuracy [28].

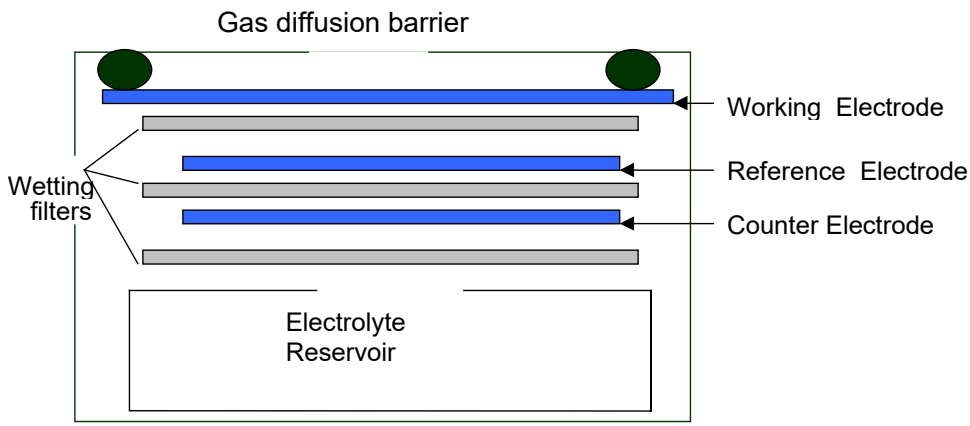

Figure 6: Diagram over a three electrode electrochemical sensor.

Disadvantages of electrochemical sensors include: cross sensitivity, hard to calibrate and reliability of the sensor. Cross sensitivity is how much the sensor react to gases besides the target gas. Electrochemical sensors measuring NO_2 have a significant cross sensitivity with O_3. A concentration level of 3 ppb, 6 µg/m^3, O_3 is enough to notably alter the measurements of the Alphasense NO2-B43F (Alphasense, Essex, United Kingdom), a top of the range electrochemical sensor for NO_2, according to a semester thesis by Balz Maag, ETH, Zürich, Switzerland [20]. The cross sensitivity with O_3 is one of the major problems with NO_2 electrochemical sensors and not only for the Alphasense sensor. Temperature and humidity are also factors affecting the performance of the sensor. Temperature affects the sensitivity, response time and the zero-offset voltage. Fast changes of temperature cause transients in the measured current because of the physical changes of the sensor body and the electrochemistry. Humidity changes have similar effects as the transients from the temperature. Temperature and humidity together also have an impact on the lifespan of the sensor. The electrolyte inside the sensor will lose or absorb water

depending on the ambient humidity. When the humidity is too low the sensor will dry out, and when it is too humid the sensor will absorb too much water and risks leaking electrolyte [29]. The process is further accelerated by the temperature. In normal circumstances an electrochemical gas sensor will last around 2 to 3 years, but with stable humidity and temperature levels the lifespan can be longer [30]. The many disadvantages, and that they are environmental, makes it very hard to calibrate. One calibration in a location might not work in another location because of environmental differences [19]. The changes that occur with the sensor when exposed to these factors are directly involved with the measurement process making it hard to estimate the deviation, thus hard to prove the reliability of the sensor.

4.2 PM measurement

PM is a notion for solid and liquid matter freely hanging in the air. It is often associated with being a decay product of combustion, but other matters such as pollen and dust is also included in the notion. Particles come in many sizes and shapes. The ones that are that are less or equal to 10 µm is small enough to get into the lungs and can cause health problems [31]. $PM_{2.5}$ and PM_{10} are the quantities that the European Union is using for air quality standard regulations, refer to 3.4 for definitions.

Naturvårdsverket, Swedish Environment Protection Agency, has regulations for how PM values should be acquired. Instruments using the reference method or instruments using a method that gives similar results to the test method is allowed [32]. The reference method should follow the standard declared in SS-EN 12341:2014. Summarised the measurement method involves physically filtering out the particles in the desired range and then weighting them manually. Doing this correctly gives very accurate results but real-time data from continuous measurement are not possible [33]. There are instruments with methods allowing real time sampling that gives similar results to the test method. According to Naturvårdsverket regulations regarding AQM, PM levels should be measured with the reference method, for example tapered element oscillating microbalance 1405F or Fidas 200. A complete list over units approved by Naturvårdsverket can be found at the web-page of the national laboratory of Sweden [33].

4.2.1 Optical Particle Counters (OPC)

OPCs count and estimates the size of particles passing through an air flow. One application they are used for is classifying clean-rooms. The technology has also become common in low-cost sensors for PM measurements. In low-cost sensors assumptions are being made about the particles shape and densities to be able to convert to particle mass.

Several detection methods can be used for detecting and measuring particles; one of them is light scattering. Many low-cost sensors including Shinyei PPD42NS (SHINYEI Technology Co., LTD, Kobe, Japan) and Alphasense OPC-N2 is using

this technology. In simple terms the setup consists of a laser beam passing through an air-flow and a photo-detector located perpendicular to the beam. When a particle passes through the beam the light scatters and some of it hits the detector. The particle diameter can be calculated from the intensity of the light by assuming the particle is spherical and the refractive index is known using Mie scattering theorem [34].

Since assumptions about the refractive index, the shape and the density of the particle must be made to estimate the particle mass, the calculated result can deviate a lot depending on the properties of the measured particles and the ones used for calibration.

5 Sensor selection

An investigation of low-cost sensors that could be integrated in a camera was made. Parameters considered when making the selection were primarily resolution and cross sensitivity. Resolution in terms of sensors defines the smallest detectable change in a quantity. The limit for what is detectable is not fixed, but is based on signal to noise ratio and the sensors response to measured quantity changes. Cross sensitivity describes the response to other gases besides the target gas. For example, an NO_2 sensor has cross sensitivity with O_3 when O_3 affects the measurements of the NO_2 sensor. For NO_2 measurement a couple of MOS and electrochemical sensors were found that matched the base criteria. The resolution of MOS-sensors is not high enough for AQM-applications. At last, two electrochemical sensors were remaining: Alphasense NO2-B43F and SPEC Sensors (SPEC Sensors, LLC, Newark, CA, USA) NO2 sensor. According to their specifications both should be able to detect NO2 resolution at concentrations around less than 20 ppb[35][36]. Both manufacturers have designed a custom sensor board to their sensors to make it easy to acquire measurements. Alphasense sensor board is analogue and according to the data sheet the noise from NO2-B43F together with the sensor board is 15 ppb. SPEC sensors offers a digital sensor board with a resolution of 20 ppb. In terms of performance the Alphasense package is able to achieve higher resolution because of the lower noise. In addition to this an analogue board gives more freedom to work with the signal processing. Both sensors have a considerable cross sensitivity to O_3, to minimise the impact of O_3 both of the sensors have an O_3 filter integrated. Results from the ETH-study[20] shows that the O_3 still can have a large impact on the result when exceeding a concentrations exceeding 3 ppb.

Four interesting candidates were also found for PM measurement, all of them are based on optical scattering to make an estimation of the particle mass. In the cheaper price range at around 200 SEK are Shinyei PPD42NS and SDS011, and the more expensive ones are Alphasense OPC-R1 and OPC-N2.

Shinyei PPD42NS is the cheapest one which is also reflected in its construction, instead of a fan it uses a resistor as a heating element to create airflow through the measurement volume. The light source is an IR-led and to get a spot measurement a lens is used [37].

The other three sensors are more alike, using laser scattering and a fan to maintain the air-flow. A German study shows that both OPC-N2 and SDS011 perform well at PM2.5 measurements. In certain conditions, OPC-N2 does perform more like the reference instrument with PM_{10} measurements [38]. At the time when this project was initiated OPC-R1 was not available for evaluation. According to Alphasense the OPC-R1 is supposed to perform like OPC-N2. With a lower price tag, smaller size and lower power consumption it would have suited well for the network camera application [39]. To get an idea of how OPC-R1 performs the final decision became to evaluate OPC-N2.

6 Hardware

This section describes the different hardware used. The main goal was to use the I/O port of the camera to power the measurement units. There were two prototype stages during the development of the NO_2 sensor-unit, the initial and the final prototype. The purpose of the initial prototype was to get data of the sensors as early as possible. The NO_2-initial prototype used socket-socket cables to connect the different evaluation modules of the chosen components for the final prototype. During the data collection the final prototype was developed. More concern was placed in minimising the noise of the NO_2-unit by eliminating unnecessary cables and evaluation modules were not used. A Printed Circuit Board (PCB) was built to achieve that. A diagram of the final setup can be seen in figure 7

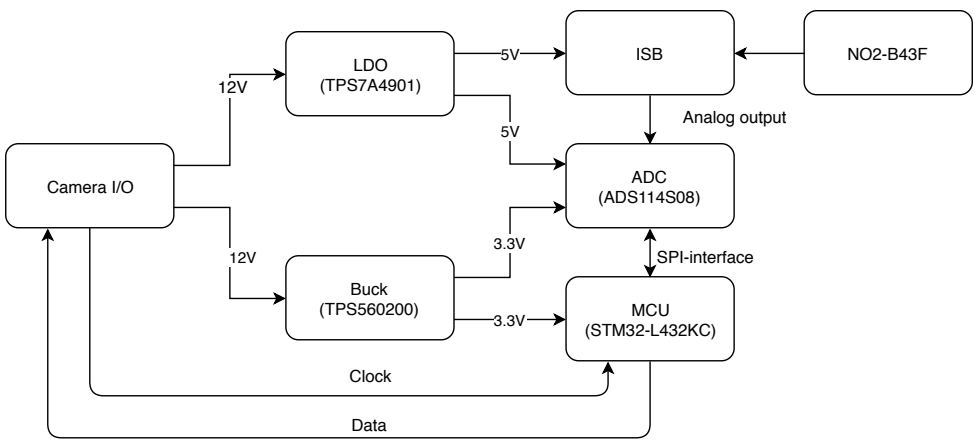

Figure 7: Overview of the NO2 box

The OPC-N2 was evaluated without being connected to the camera. A simple measurement setup using the MCU as a link to the computer and a USB-power supply was used.

6.1 Camera I/0

Some network cameras are equipped with an I/O-port. The purpose with this port is to be able to control external equipment such as relays, lamps and trigger events based on signals from switches and sensors.

The connectors for the I/O-port differs depending on the camera model. In this project a network camera with a four-pin configuration: ground, 12 V DC, input and output, was used. The 12 V DC output are specified to deliver currents up to 25 mA. The input and output have a pull-up transistor configuration which makes them versatile and independent of which voltage that is required by the external

equipment. The pull-up output configuration can be supplied by either an internal 12 V source by connecting an external voltage supply to the output connector.

6.2 STM32-L432KC

STM32-L432KC is a development board similar to an Arduino, based on a STM32-L432KCU6 Micro Controller Unit (MCU). The STM32L432KCU6 delivers an excellent power to performance ratio with 84 µA/MHz [40]. As comparison, ATmega328/P which is used in Arduino Uno requires 200 µA at 1 MHz running speed [41]. The board has a lot of connection opportunities including 2 SPI-interfaces, a 12-bit ADC and several pin-outs with PWM compatibility.

6.3 Alphasense OPC-N2

Figure 8: The Alphasense OPC-N2. The dimension of the sensor is about 70 x 65 x 60 mm.

OPC-N2 is a compact low-cost particle counter, Figure 8. It works according to the light scattering principle explained in 4.2.1. OPC-N2 measures does its measure in an open scattering chamber instead of a narrow inlet. The reason for using a narrow inlet is that it reduces the risk for multiple particles scattering the laser at the same time and get invalid results. A narrow inlet lead to a pressure drop and requires a powerful air-pump to get a decent airflow. The drawback of this is that the pump requires power and maintenance. To reduce the problem with multiple particles scattering at the same time and maintain a high efficiency Alphasense have created a virtual sensing zone. The principle of their virtual sensing zone is described in their patent [42]. The virtual sensing setup consists of an elliptical mirror and a dual-element photodetector, see Figure 9. The elliptical mirror is placed in a way that the virtual sensing zone gets focused in the inner part of the photodetector. If 25 % or more of the total measured scattered light is detected by the inner photodetector the scattering is considered to come from a particle inside the detection area, in other case the measurement sample gets discarded.

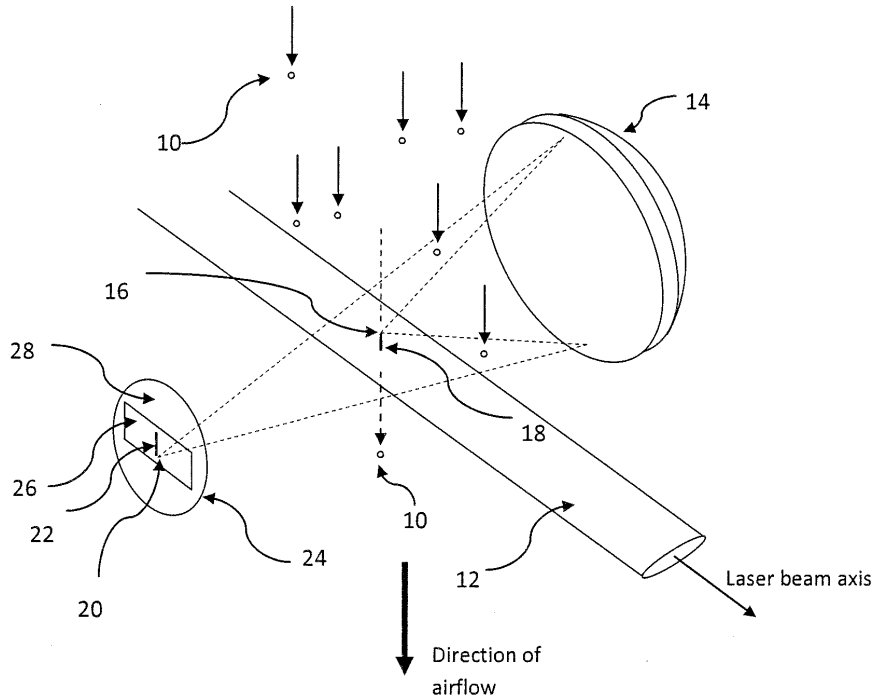

Figure 9: Drawing of the virtual sensor zone setup. The drawing is taken from Alphasense patent documentation [42].

The particle size is estimated using Mie scattering, assuming an average refractive index of 1.5, spherical particles and knowledge of that the laser wavelength is 658 nm. With this estimation the particles are being categorised in 16 size bins in a range between 0.38 µm and 17 µm . From the size distribution the PM values are being calculated with a method defined by the European Standard EN 481. The method involves weighting the different size-bins with a factor defined by the EN 481 standard and multiplying each bin with a particle density factor. By default, this value is 1.65 g/ml. Each OPC-N2 is also calibrated before shipping which gives an additional weighting factor.

OPC-N2 has a 6-pin pico clasp male Molex for SPI communication and a micro-USB to access the internal SD card storage. The 6-pin have the following pins for SPI communication with the VCC-pin closest to the USB-port: VCC, SCK, SDO (MISO), SDI (MOSI), SS (CS), GND.

The power needed for operating the OPC-N2 is 4.8 to 5.2 V and 175 mA continuous current. The power can be feed from the USB-port or by using the VCC-pin. The SPI logic lines only accept 3.3 V [43].

6.4 Alphasense NO2-B43F with Individual Sensor Board

Figure 10: The Alphasense line-up of NO_2 and O_3 electrochemical gas sensors. The B-series sensors has an diameter of 32 mm

The Alphasense NO2-B43F, seen in Figure 10, is a 4-electrode electrochemical gas sensor designed to be more robust in outdoor environments than the A-series electrochemical sensors from Alphasense. The 4-electrode system differentiates the NO2-B43F from the more conventional electrochemical sensors, which only use three electrodes. The fourth electrode in NO2-B43F is the auxiliary electrode and has the function to provide an accurate way to measure and subtract the zero-offset voltage from the measurements. As temperature, humidity and other environmental factors changes the zero-offset voltage will also follow. With the auxiliary electrode these changes are considered and, in paper, able to increase the accuracy. Besides the fourth auxiliary electrode the other three electrodes: working, counter and reference electrode, fulfil the same roles as a conventional 3-electrode electrochemical sensor described in 4.1.1.

A conventional 3-electrode electrochemical sensor uses the reference electrode to set a fixed voltage potential on the working electrode to get the desired characteristics, and so do the NO2-B43F sensor from Alphasense. As the potential of the working electrode deviates from the reference, additional current must be absorbed or delivered to the counter electrode to keep the potential stable at the working electrode. One way to achieve this is by using a potentiostatic circuit. Alphasense develops and uses their own potentiostatic circuit with additional amplifiers to give a voltage output that relates to the gas concentration and to keep the noise down. If the sensor is ordered together with the circuit, Individual Sensor Board (ISB), then the ISB is factory calibrated to that specific sensor. Our sensor was ordered together with the ISB and the calibration values are found in Table 1. The sensitivity value was used to calculate the mass concentration of NO_2.

Interfacing with ISB is with a 2.54 mm 6-pin Molex header socket. The meas-

urement values in voltage are accessed through the OP1 pins, which are converted from the current flowing through the working electrode. OP2 pins corresponds to the auxiliary electrode and are used to measure the zero-offset voltage. Power to the ISB is supplied through the +VIN and -VIN pins and ground is shared between all the negative pins. It is possible to only use four pins and still maintain the full functionality of the ISB, but due to electromagnetic interference concerns it is still advantageous to use all six pins and route them in pairs. The ISB requires is a stable voltage in the range between 3.5 to 6.4 V to deliver a noise free signal. Preferably from a separate power supply with no noisy circuits shared. Decoupling capacitors are also recommended by Alphasense themselves [44].

Table 1: Calibration values provided by Alphasense UK.

Gain (mV/nA)	-0.73
WE Zero (mV)	243
Aux Zero (mV)	241
WE Sensor (nA/ppm)	-377
Sensitivity (mV/ppb)	0.275
Electronic Zero WE (mV)	281
Electronic Zero Aux (mV)	256

6.5 Texas Instruments ADS114S08 16-bit sigma-delta ADC

The Texas Instruments ADS114S08 is a 12 channel, 16-bit, delta-sigma Analog-to-Digital Converter (ADC). The high resolution allows accurate measurements below 1 V. Using the internal voltage reference of the ADC, 2.5 V, with gain setting 1 will give a resolution of:

$$\text{Resolution (V)} = \frac{V_{\text{ref}}}{2^{\text{bits}}} = \frac{2.5\,\text{V}}{2^{16}} = 38\,\mu\text{V}, \tag{1}$$

in single-ended measurements. Given the noise from the datasheet of the ISB for NO_2 is 15 ppb, the required resolution would be:

$$\text{Noise (ppb)} \cdot \text{Sensitivity (mV/ppb)} = 15 \cdot 0.275 = 4.125\,\text{mV}, \tag{2}$$

which are within the resolution of the ADC. With shielding and digital smoothing the noise can be further reduced.

The analogue section of the ADC require noise free and stable unipolar 2.7 to 5.25 V or bipolar $\pm$2.5 V. The digital and IO section requires 2.7 to 3.6 V. It is recommended to keep the power supply of the analogue section and digital section separate [45].

6.6 Texas Instruments TPS7A4901 low-dropout voltage regulator

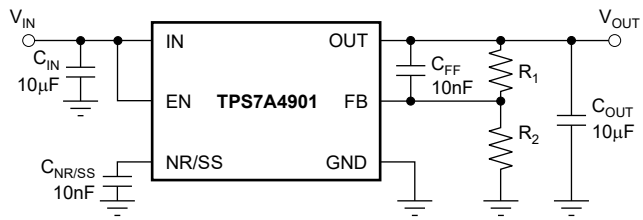

Figure 11: A typical layout of the TPS7A4901. There are one additional pin on both sides that are neglected in the diagram as these pins are not relevant to the operation of the regulator.

The Texas Instruments TPS7A4901 is a Low Dropout (LDO) linear voltage regulator made for sensitive applications such as powering an analogue section of an ADC. The nature of the LDO regulator has other advantages such as low electromagnetic interference and filtering out ripples of the power supply. There are disadvantages with an linear regulator compared to a buck-converter. One of them is efficiency and during the conversion the energy of the conversion are released as heat. The energy dissipated are related to the difference between the supply voltage and the output voltage, and the current draw from the regulator.

The input voltage of the LDO regulator ranges from 3 V to 36 V with and configurable output of 1.194 V to 33 V. The output is set by two resistors, R_1 and R_2, in Figure 11. The output of the linear regulator is determined by Equation (3), with $V_{\text{FB(nom)}}$ being typically 1.185 V [46].

$$V_{\text{OUT}} = \left(\frac{R_1}{R_2} + 1 \right) V_{\text{FB(nom)}} \tag{3}$$

6.7 Texas Instruments TPS560200 synchronous step regulator

When the current draw is high and the differences in supply voltage and output voltage is big it is generally more efficient to use a buck converter, such as the Texas Instruments TPS560200, for down conversion. Buck-converters generate noise, so it is not suitable for sensitive electronics and should be kept well isolated. The efficiency of the TPS560200 is dependent on the amount of current drawn and has a rated 500 mA continuous output current. From an input between 4.5 to 17 V the voltage is down converted to a configurable output voltage between 0.8 to 6.5 V. The output is configured by changing the ratio between the resistors, R1 and R2 in Figure 12 and are calculated by the following Equation (4) [47].

$$V_{\text{out}} = \frac{\text{R1} \cdot 0.8\,\text{V}}{\text{R2}} + 0.8\,\text{V} \tag{4}$$

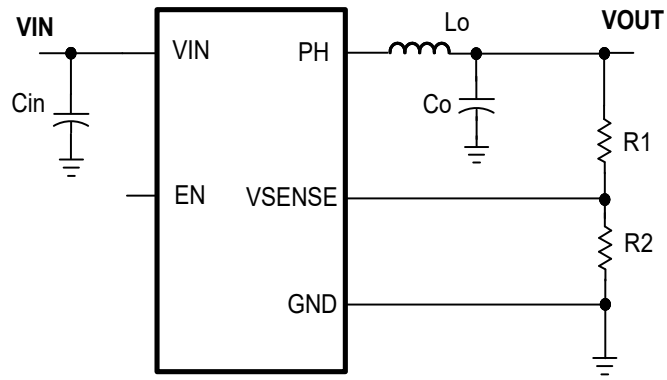

Figure 12: Simplified schematic of the TPS560200.

6.8 Initial prototype configuration

An initial prototype was built to get measurement data as fast as possible. Therefore, many decisions that were made were not ideal for minimising noise and reliability. The hardware used in this prototype were mostly Evaluation Module (EVM) of the previous mentioned hardware. The EVM for the ADC was ADS114S08EVM and for the LDO regulator it was TPS7A30-49EVM, which also contained a TPS7A30 LDO regulator besides the TPS7A49. The part with TPS7A30 was broken away to save space. A similar buck-converter to the TPS560200 was used as the EVM of the mentioned buck-converter was readily available. The EVM used was a TPS54061-EVM, which contains the buck-converter TPS54061.

Figure 13 describes the power flow of the whole set-up. A self-made battery-pack consisting of two parallel connected four AAA battery was used as the main source of power and was fed into the LDO regulator and buck-converter. The analogue section of the ADC was powered by the 5 V rail from the LDO regulator while the digital and logic sections were powered by the 3.3 V rail from the buck-converter.

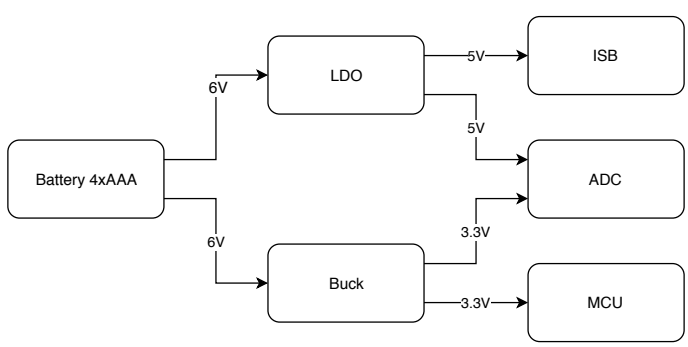

Figure 13: The power diagram of the initial prototype.

The ADC evaluation module, ADS114S08EVM, was provided by Texas Instruments. The main component of the module was the 16-bit sigma-delta ADS114S08 ADC. As it was an evaluation module many components were already pre-installed to get the utmost of the ADC and to simplify the evaluation process. The MCU, external voltage reference, external power supply that were pre-installed were bypassed to allow a better representation with the chosen components used in the final prototype.

Power to the ISB was fed from the battery and down-converted by the LDO regulator. From the factory the EVM for the LDO regulator was configured to 15 V output which were not useful in this case and were re-configured to 5 V output. The re-configuration meant changing a resistor in the EVM, Figure 14, labelled R_4.

The pre-installed resistor R_3 and R_4 had a resistance of 604 kΩ and 51.1 kΩ respectively. The resistor R_4 was determined to 188 kΩ by using the Equation (3). R_1 was R_3 and R_2 was R_4 in the referred equation [46][48].

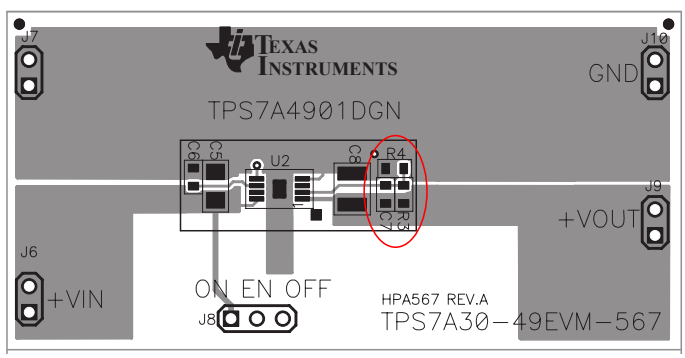

Figure 14: The EVM provided by Texas Instruments. The board has two LDO regulator but only TPS7A4901DGN was used. The SMD resistors marked are the feedback resistors used to determine the output voltage.

The TPS54061EVM, buck-converter EVM, was pre-configured to have an output voltage of 3.3 V and has an enable pin to shut down the buck-converter when the input voltage is below a certain voltage threshold. Because the factory setup did not start the regulator for input voltages below 7.5 V, the resistance, R2, was increased to 50.4 kΩ to decrease the voltage threshold [49].

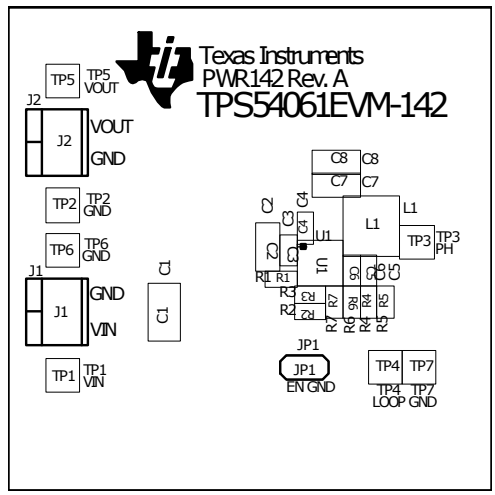

Figure 15: The board layout of the TPS54061EVM. The buck-converter is labelled as U1.

6.8.1 Enclosure

The initial prototype was placed alongside a reference measurement station in an outside environment. Being outside meant an enclosure was needed to protect the components and to make the unit portable. An aluminium die cast box by RND Components was bought and modified to accommodate the needs of the prototype. The dimension of the box was 112 x 62 x 31 mm, Figure 16 [50]. The top of the box was drilled to fit and expose the gas diffusion membrane of the NO_2 sensor. The gap between the sensor and the hole was sealed with sealant to keep dust and water from the components. An iron sheet metal roof was constructed to keep rain from direct contact with the sensor membrane. Because aluminium and iron oxidises with air a thin piece of Polytetrafluoroethylene (PTFE) was glued on the surface closest to the sensor and on the inside of the roof to minimise the disturbance of the oxidation. The whole prototype is shown in Figure 17.

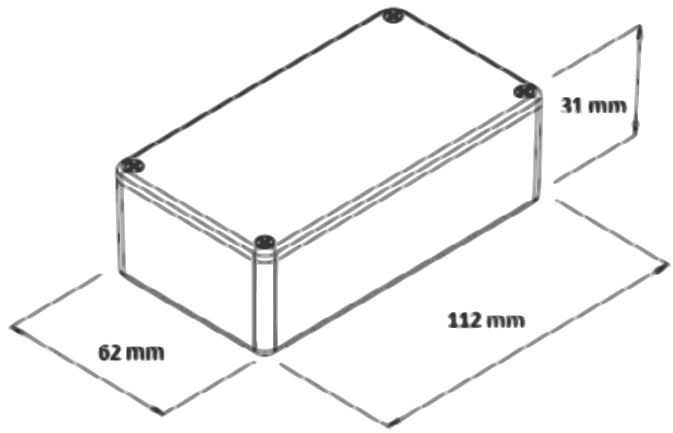

Figure 16: The aluminium box used in the initial prototype. This was later modified to accommodate the sensor requirements.

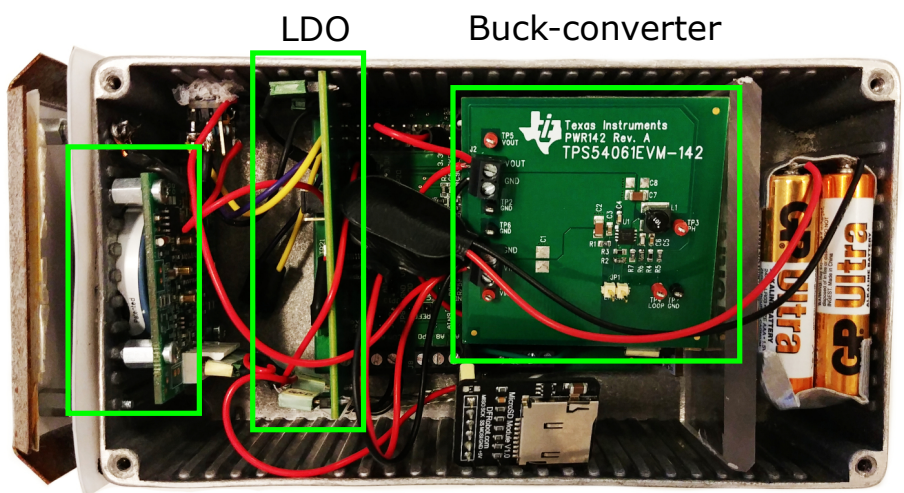

NO2-B43F with ISB

Figure 17: The initial prototype with the lid off. Underneath the buck-converter sits the ADC and MCU. Besides the buck-converter is the SD-module used to log the measurement data. The PTFE pieces can be seen as white sheets inside the roof and the top of the box. The roof has started to rust, because the box has been sitting outside.

6.9 Final prototype configuration

The final prototype included improvements to minimise noise over the initial prototype that was developed during the tests of the initial prototype. The improvements

were; elimination of cables, more compact enclosure and a self-made PCB that acted as a data acquisition board. The power flow of the whole system is similar to the power diagram of the initial prototype in Figure 13. The only difference is the power source, which is 12 V from the camera.

A schematic was drawn for the PCB. The buck-converter TPS560200 was simulated in Texas Instruments WEBENCH® and the schematic for the buck converter was generated from the simulation. The schematic of the LDO regulator, TPS7A49, followed the schematic shown in the section 9.2 Typical application in the data-sheet [46]. In a similar way the schematic of the ADC was a modified version of what could be found in 10. Application and implementation in the data-sheet for ADS114S08 [45]. The whole schematic is found in Appendix A.

6.9.1 PCB

A PCB was designed to minimise noise and make the whole package more compact. The PCB was designed in 4 layers with the bottom side used for digital and noisy signals, the inner bottom layer for power planes, the inner upper layer for ground plane and the top layer for analogue signals. A rough layout diagram is shown in Figure 18. The buck-converter and the contacts for MCU and the I/O-port was placed on the bottom side of the PCB. The power planes are divided into 12 V+, 5 V+ and 3.3 V+. On the top layer sits the ADC, LDO regulator and the contacts for the ISB of NO2-B43F. The complete PCB layout is found in Appendix B.

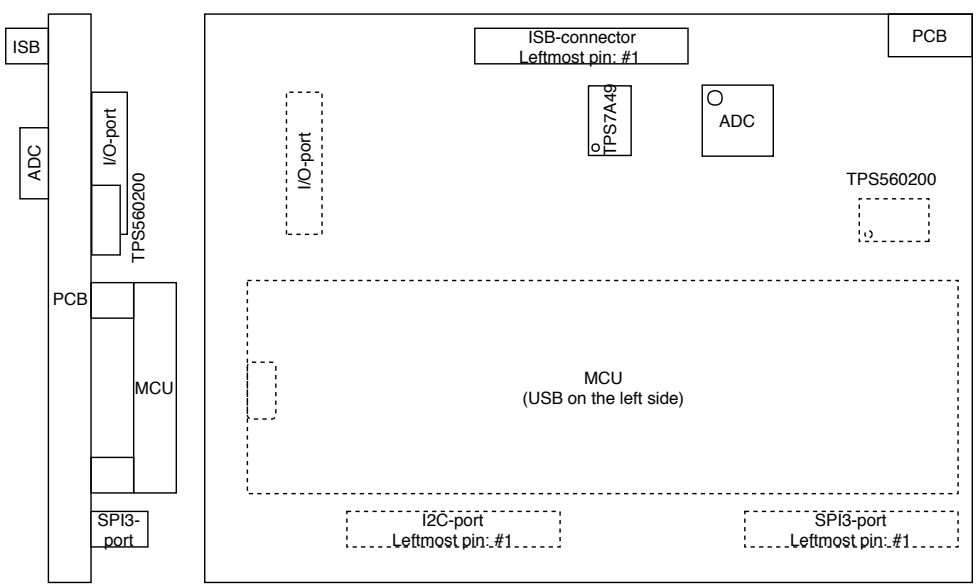

Figure 18: The rough layout of the PCB-layout showing the components placement.

6.9.2 Enclosure

A smaller enclosure with the dimensions: 92 x 92 x 42 mm, was used, Figure 19. The enclosure was manufactured by Hammond Manufacturing Co. Ltd. and was made of aluminium. A gasket was included and the provided screws had an O-ring for added protection against fluids.

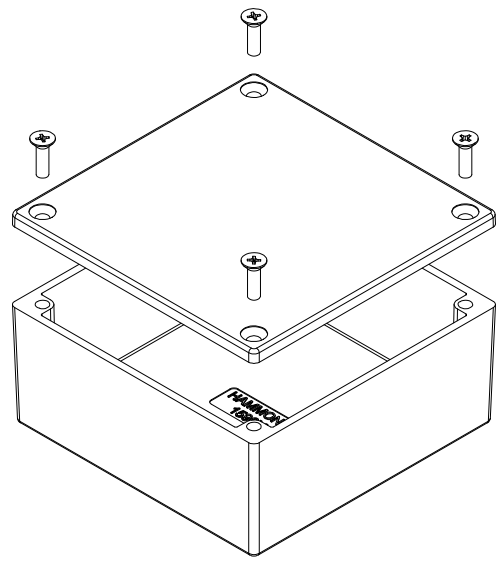

Figure 19: The enclosure used for the final prototype.

The back of the box was drilled out to allow the sensor to protrude. A roof was also made from cut and bent sheet of copper. Inside the copper roof, sheets of PTFE was glued on. Once the necessary holes for screws and cable gasket were drilled, the box, roof and the lid were painted white. The sensor was sealed with the same sealant used in the first prototype and is shown protruding out of the of in Figure 20. The gasket was installed and the overview of the final prototype is shown in Figure 21.

Figure 20: The side-view of the box with the NO2-B43F sensor installed. The lid of the enclosure is faced downwards.

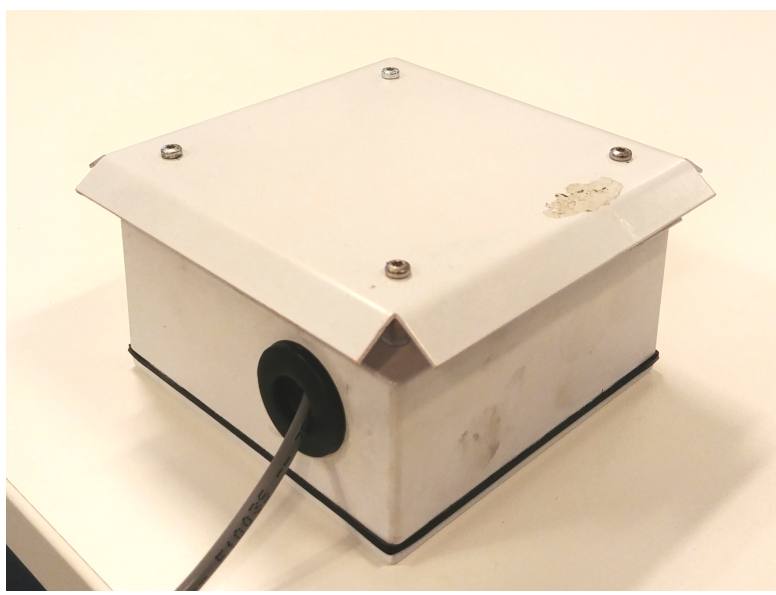

Figure 21: An overview of the final prototype.

7 Software

One of the key targets with the project was to use the camera as an interface between internet and the measurement unit. To be able to achieve that a custom link between the cameras I/O interface and two digital I/O pins on the microcontroller was set up. The camera sends a clock signal which triggers the microcontroller to return a digital bitstream. The data are retrieved from the built-in SFTP-server of the camera via internet.

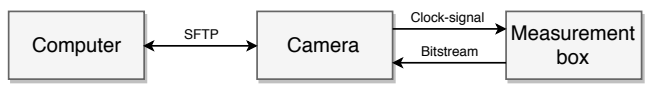

Figure 22: Communication schedule

7.1 I/O communication

The I/O communication consists of two parts: a bash script running on the camera for sending a clock signal and receiving data, and code on the microcontroller that sends bits when requested by the camera.

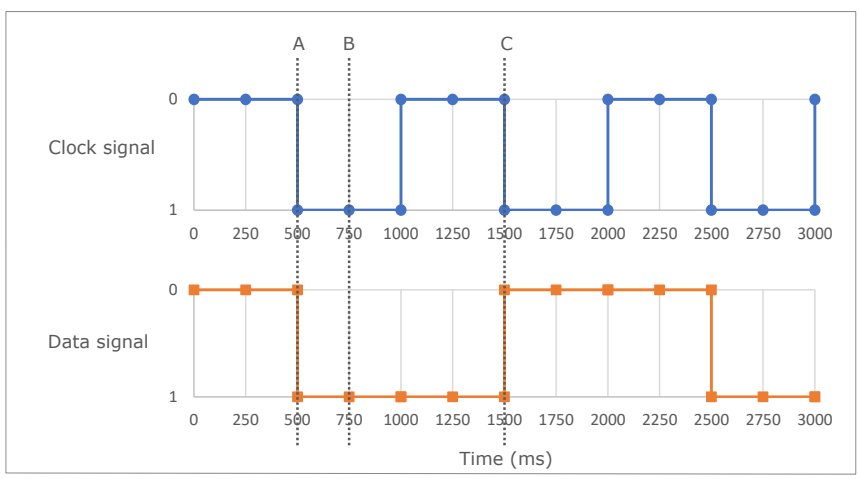

Figure 23: The graph demonstrates the pattern for sending a bit sequence containing ”101”. Further comes a description of the moments marked in the graph. A) The clock signal falls which triggers the microcontroller to change its output value corresponding to the next bit in the queue B) At the middle of the clock signal the camera reads the value of the microcontroller output. C) The microcontroller gets triggered again and changes its output value to next bit in the queue.

MCU

The latest reading value is stored into a 48-bit bitset containing voltage for the work-

ing and auxiliary electrode and a checksum for each value. The bitset object makes it easy to read and edit single bits from a dataset. When the microcontroller detects an falling edge in the clock function an interrupt is calling a send function. The send function reads a bit from a location in the bitset addressed by a counter, writes the bit value on the output and then increases the counter value by one. After 48 clock cycles the whole dataset has been sent and the counter resets.

Bash code
The camera-OS has a built-in function that can control and read the I/O port. By using a function controlling the port and the cameras built-in delay functionality, a script with the behaviour described in figure 23 could be achieved. The script stores the reading values in a file located on the camera's SD-card.

Computer
A python script was written to visualise the collected data in real time. The script collects bit sequences continuously from the camera, converts it to decimal numbers and makes a plot of them. To make sure that the data is valid the bitset is checked against the supplied CRC-checksum.

7.2 Optical particle counter

OPC-N2 communicates in the same way as most SPI devices. The SPI master sends a byte and OPC-N2 replies with a byte, between each byte transfer there should be a specific delay. Available commands and their associated transaction sequence can be found in Alphasense SPI information document for OPC-N2 [51].

A Ph.D. student at MIT have made a C++ library available with functions for reading and configuring the OPC-N2 [51]. This library has been used as a base for the controlling the OPC with the microcontroller. Since the code was initially made for a Particle Photon board (Particle Industries, Inc., Minneapolis, United States) some modifications have been made to fit the Mbed syntax and definitions.

The library was used for a simple sequence that basically just pulls data from the OPC and forwards it to a computer. The flow for the microcontroller code can be seen in Figure 24.

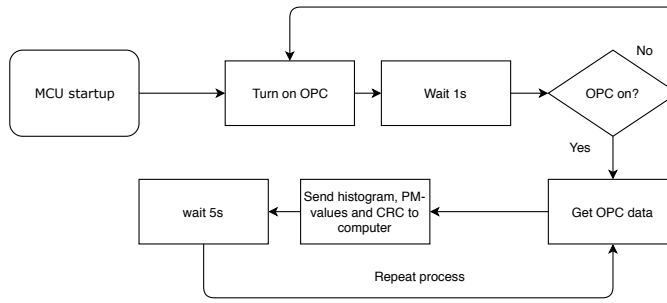

Figure 24: Flowchart over the OPC-code for the microcontroller

8 Evaluation

This section describes the evaluation process of each sensor unit. Three tests were performed with the Alphasense NO2-B43F with the purpose of investigating the behaviour of the electrochemical sensor. One of the tests used a climate chamber to expose the sensor with a controlled temperature and humidity and the two other tests were outdoor tests next to a reference measurement station. The initial prototype was used in both the climate and outdoor test while the final prototype was used only in the outdoor test in Malmö, because of time constraints. Measurement data was later retrieved from the reference measurement station. The PM sensor, OPC-N2, was evaluated by comparing it with two other instruments in an open outdoor environment.

In the EPA Air Sensor Guidebook [22] precision and bias are used as the criteria to evaluate air quality sensors. Depending on the performance they categorise the sensors into different tiers. The aim for this thesis was Tier 3: Supplemental Monitoring, which requires a precision and bias error of less than 20 %. According to the guidebook precision is calculated with the following equation:

$$P = \frac{C_s}{C_m}. \tag{5}$$

P is the precision, C_s is the standard deviation of the measurement and C_m is the mean value. Precision measurement is done when the target quantity of the sensor is held constant. In this thesis the precision tests were excluded since the required test environments were not available. As for the bias, the following equation was used:

$$B = \frac{C}{C_R} - 1. \tag{6}$$

B stands for bias, C for the average of the measurements of the sensor C_R for the average of the reference in the same period.

To give an indication about how the sensors performs, both least squared and Deming regression analysis was performed. Compared to least square regression, Deming regression also take into consideration that the reference instrument has a standard error. Ideally the ratio, δ between the instrument variances should be used when making the Deming estimation. Since variances for the instruments used in the evaluation are unknown the ratio is set to 1.

8.1 Test set-up

Various equipment were used in the tests and the location of the test varied as some equipment were only available in that location. The test set-up for the different tests are presented in this section. Three different test set-up was used for testing the NO2-B43F and one set-up for the OPC-N2.

8.1.1 NO_2: Climate test

The set-up for the climate test consists of a climate chamber from CTS (CTS GmbH, Hechingen, Germany) and a power supply for the sensor unit. The test was divided into two parts. Humidity was held constant at 50 % while 5 °C step change was made every hour from -10 to 30 °C in the first part. In the second part the temperature was held constant at 20 °C while 10 % step changes were made every hour from 10 to 90% relative humidity. The sensor unit was placed in the centre of chamber and powered by a external power supply. All the measurements from the sensor unit is logged internally on an SD-card.

8.1.2 NO_2: Initial prototype outdoor measurements

Outdoor measurements were performed alongside a reference measurement station. The initial prototype was put inside a cage on top of the station, Figure 25. As the prototype was battery driven no additional power cable was needed. This particular measurement station uses a DOAS instrument, OPSIS AR500 (OPSIS GmbH, Frechen, Germany), to measure the components in the air and the units of the DOAS are shown in Figure 26 and 27. The light source sends a beam of light to the reflector. The light reflects back from the reflector to the receiver, which are in the same unit as the light source. Based on how much light is absorbed, the different components can be determined. The test went on until the batteries were consumed.

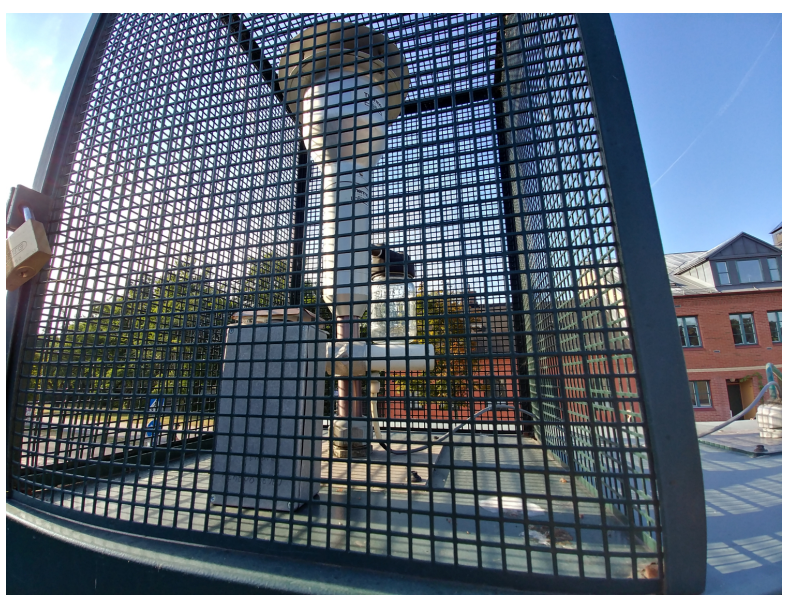

Figure 25: The small aluminium box in front of the air intake is the initial prototype used for measuring NO_2. The air intake is used for the tapered element oscillating microbalance instrument to measure particle mass concentration, which was not considered in this test.

Figure 26: Light source of the DOAS. The light is created from a tungsten tip. In the same unit is the photodetector to receive the light from the reflector.

Figure 27: The purpose of the reflector is to reflect the light from the light source to the photodetector. This reflector is 50 m away from the light source, which gives a total distance of 100 m.

8.1.3 NO_2: Final prototype outdoor measurements

The finalised prototype was placed in Malmö, Dalaplan, at the inlet of the measurement station, Figure 28 and 29, maintained by Malmö stads Miljöförvaltning. The prototype was mounted around the same height as the inlets of the instruments at around 3 m above the ground, Figure 30. An 8 m power cable was drawn from the prototype down to the instrument room directly under the pole and was connected to a 12 V power supply. The instrument used for measuring NO_2 was an ECO PHYSICS chemiluminescence CLD 700 AL (ECO PHYSICS AG, Duernten, Switzerland). As opposed to the DOAS in the previous outdoor measurement, the CLD 700 AL takes a point measurement. This is more comparable with the prototype as it also measures in a point, about 10 cm away from the inlet of the CLD 700 AL.

Figure 28: The measurement tower that protrudes from the ground has all the measurements station's sensor inlets for the instruments. The cables are routed directly below the ground.

Figure 29: Underneath the tower is the control room which houses all the instruments.

Figure 30: The mounted prototype can be seen inside the red circle.

8.1.4 Particle matter and particle counter comparison with other OPCs

The OPC-N2 was evaluated by making a measurement in free air together with two well known instruments. A particle counter, BioTrak 9510-BD and a DustTrak 8533 that makes an estimation of the PM concentration in the air. Both of them are using Mie-scattering to make their estimations, but can be assumed to be more precise than the OPC-N2 with an higher air-flow and narrower measurement area. The measurements were made outdoor at the top floor at one of LTHs buildings, an environment that is not very polluted. The measurements were done in two sessions. First time with both the BioTrak and the DustTrak, and the second time with only the DustTrak as comparison.

Figure 31: The measurement setup during the first experiment. The OPC-N2 was taking in air through an opening in the window to the left.

8.2 Results

The results from the tests are presented in this section along with evaluations. The standard deviations, absolute minimum and maximum error, mean error and the Deming plot are presented. The bias, which is one of the criteria used in EPA's air sensor guide book, are also presented for both the NO2-B43F and OPC-N2.

8.2.1 NO_2: Climate test

The results of the climate test were compiled into two plots, Figure 32 and 33. The first plot shows the temperature test, which was done before the humidity test, and the second plot shows the humidity test.

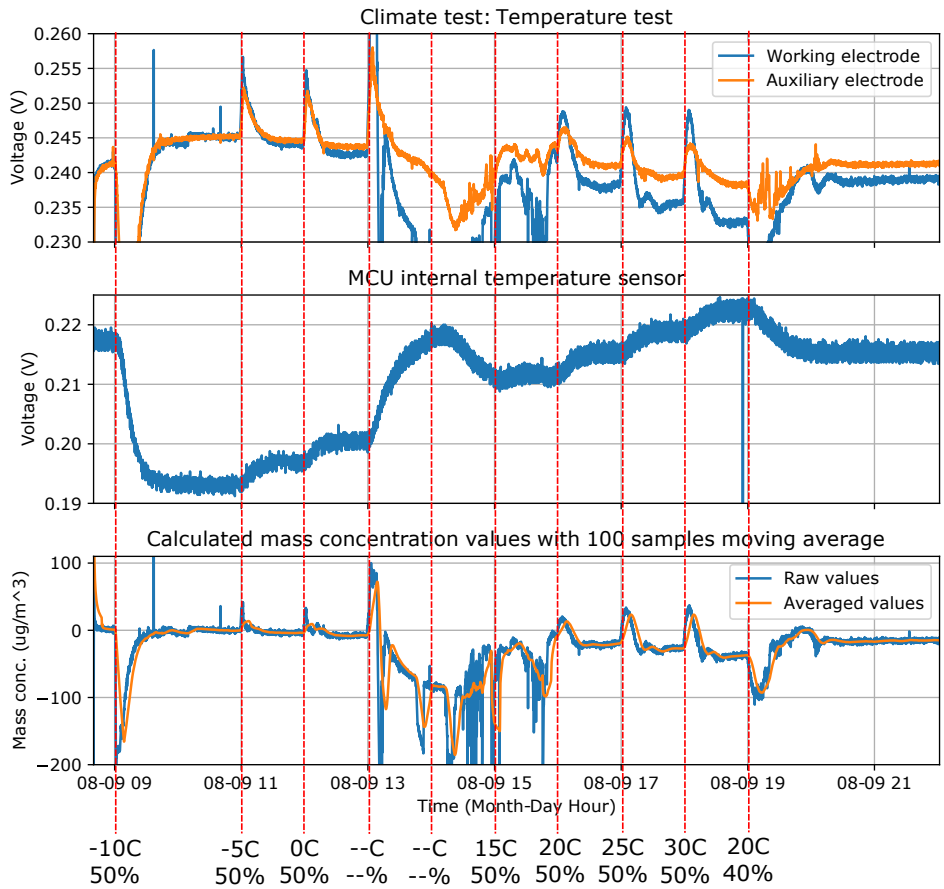

Figure 32: The measurement data logged during the temperature test in the climate chamber. The red dashed lines indicates when a step change was made in the climate chamber. The top subplot shows the voltages of the working and auxiliary electrode and the middle subplot shows the voltage of the internal temperature sensor of the MCU. The final subplot shows the calculated mass concentration of NO_2.

In Figure 32, it is clear that a sharp increase of temperature affects both the working and auxiliary electrode. Between 0 and 15 °C the climate chamber did not follow the test program, but the general behaviour of the sensor could still be observed. An increase in temperature results in a positive peak in voltage for both of the working and auxiliary electrode and the opposite is also true. The mass concentration is based on the difference of the working and auxiliary electrode, and when the temperature

changes it is observed that the effect of the temperature changes is not equal on the two electrodes. The differences are greater as the temperature rises and the peaks in the last subplot are bigger because of these.

In the non-specified region, when the test program failed to run, a decrease in voltage and mass concentration was observed when the temperature increased. This behaviour negates the previous mentioned observation with positive peaks on positive temperature steps. One parameter not shown is the humidity and was the reason for this behaviour. On the climate chamber the humidity was measured and it was shown to decrease sharply at the beginning of the non-specified region.

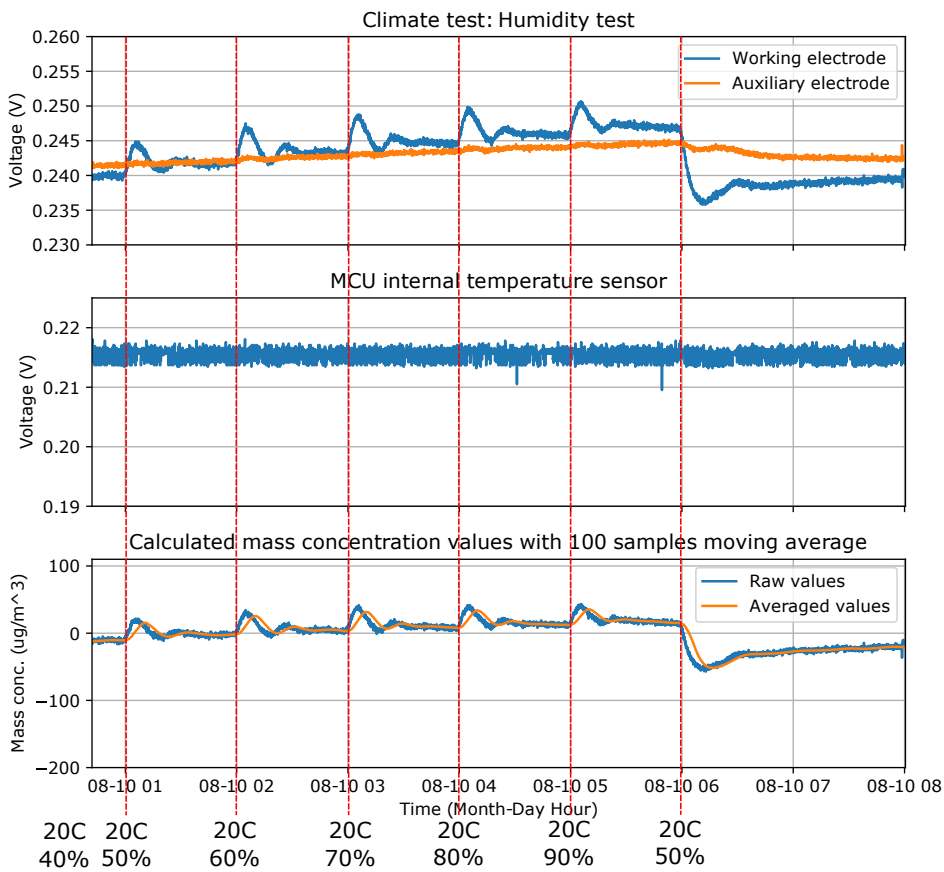

Figure 33: The measurement data logged during the humidity test. The subplots show the same parameter as in Figure 32.

After the temperature test, the humidity test started. The humidity range was planned from 10 to 90 % but the test initiated from 40 %. Like the temperature test, some data was lost but the general behaviour can still be observed. Unlike the temperature test the differences of the effect from the humidity step in the electrodes are different. The peaks only appear in the working electrode while the level of the

auxiliary electrode only rises slowly. At the end of the test a drop-off of humidity led to a large dip in the working electrode voltage. This resulted in a negative dip in the calculated mass concentration.

In the non-specified region of the temperature test, Figure 32, this behaviour is partly observed, when despite an increase in temperature, the voltage of the working electrode declines significantly more than the auxiliary electrode. As the dip of voltages is mainly from the effect of the change in humidity, it confirms that the working electrode are more sensitive to humidity changes.

As mentioned in the theory part, the sensor is known for being temperature and humidity-dependent. The results obtained coincides well with what is described in Alphasense documentation [29]. The zero current is also temperature dependent, this explains the negative offset that appeared in the temperature test. The peaks that appear with the humidity increase are also written in the documentation. The peaks in the temperature test departs from what the documentation shows and are much more intense. In the documentation they are showing the characteristics of a CO sensor which can have a bit different behaviour from the NO_2 sensor. The offset that can be seen in the humidity test does not exist on the Alphasense plot either.

8.2.2 NO_2: Initial prototype outdoor measurements

The results of the comparison with the DOAS are visualised in figure 34. A deviation up to 35.5 µg can be observed. The most significant deviations happen when the temperature changes drastically. From the climate chamber test an increase of temperature should yield a positive peak on the measurements. This was not the case as a negative peak occurs more frequently when the temperature rises. The missing information is the humidity. Rising temperature could often lower the humidity and if that is the case then the negative peak of the measurements could be partially explained.

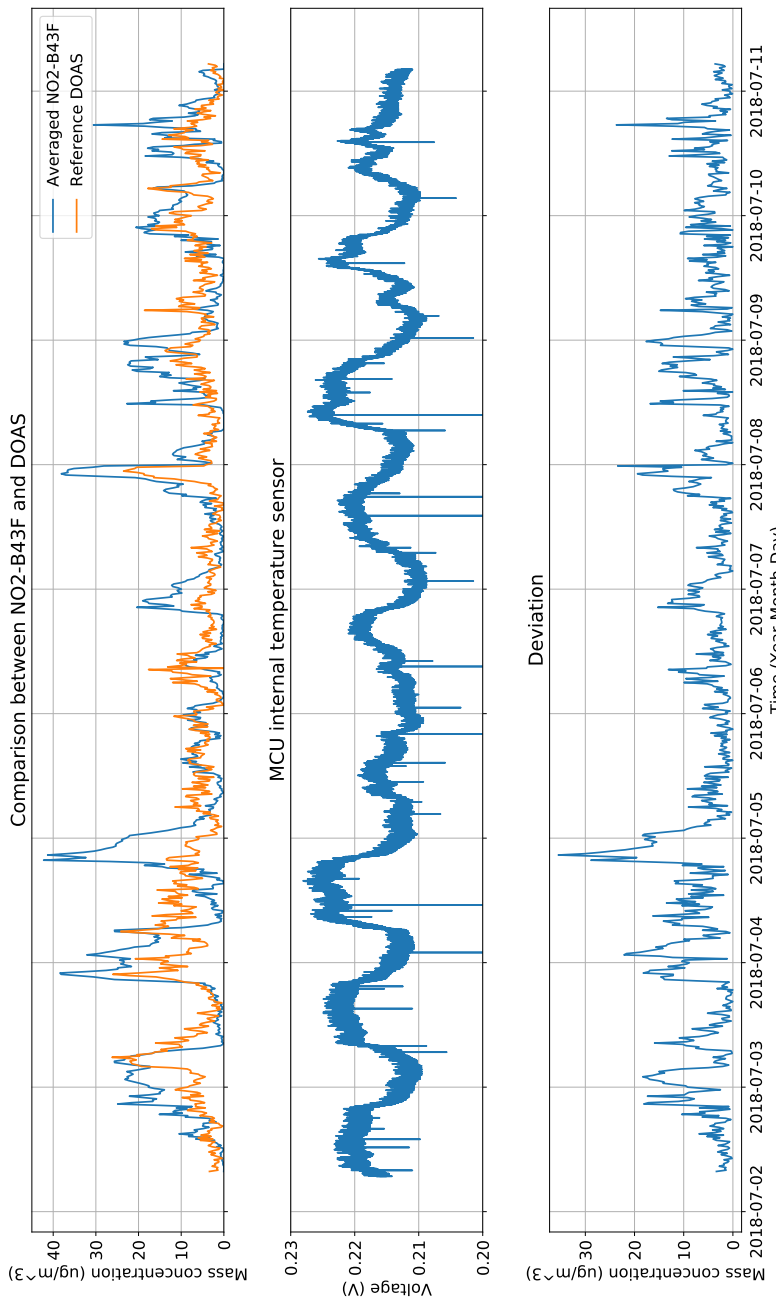

Figure 34: Results from the comparison with the DOAS. First plot shows mass concentrations for both units. Second plot shows the relative temperature measured by the internal sensor on the MCU. The third plot shows the difference between the measurements.

Some statistics from the comparison can be seen in Table 2. A calibration factor

with a first order polynomial was calculated using a curve fitting function in MATLAB. The errors with the calibration factor applied is also shown in the table. Compared to the study from Balz Maag [20] which did a similar evaluation, the mean and standard deviation of the error is significantly smaller. In this evaluation the auxiliary electrode was used unlike in the other evaluation, that could be a reason for the improved result. As mentioned before, the electrochemical sensors are affected by environmental factors, and can be a reason for the differences in results.

For the bias calculation, Equation (6), the mean was taken over the whole period of the test and the DOAS was used as the reference mean. The resulted bias error was 30 %, which is over the limit of tier 3. The Deming regression line in figure 35 shows that the uncalibrated measurements has a slight offset and a quite large systematic error. The error distribution between the Deming estimation and the real relationship is shown by the red perpendicular lines.

Table 2: Statistics of the error and bias between NO2-B43F and the reference. The numbers are based on the data from the evaluation

NO2(Lund)	Uncalibrated	Calibrated
Average absolute error	$5.5\,\mu g/m^3$	$2.9\,\mu g/m^3$
Standard deviation	$5.0\,\mu g/m^3$	$2.4\,\mu g/m^3$
Abs. error [Min, Max]	$[0, 35.5]\,\mu g/m^3$	$[0, 16.1]\,\mu g/m^3$
Bias	30 %	0 %
R^2	0.284	

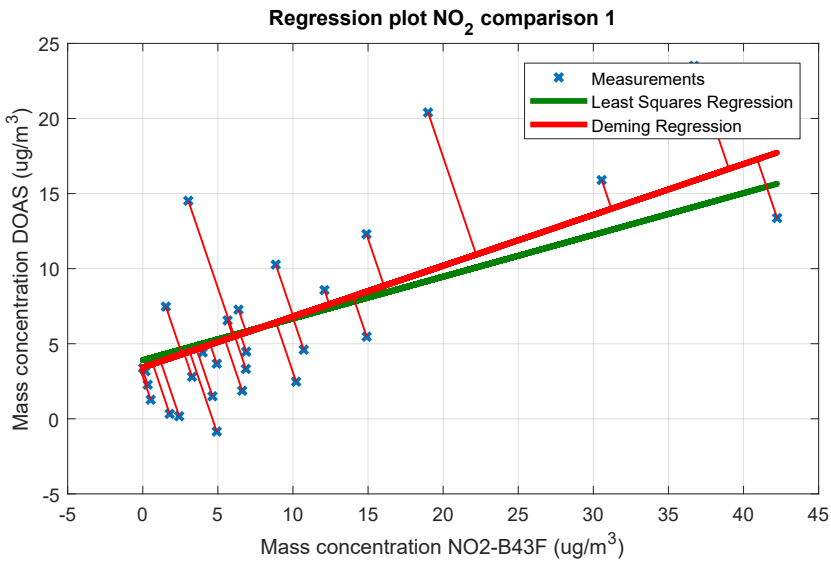

Figure 35: Plot showing estimated Deming and least square regression line with NO2-B43F on the x-axis and DOAS on the y-axis.

8.2.3 NO_2: Final prototype outdoor measurements

The duration of the outdoor measurement test in Malmö was 5 days with the final prototype. The results of the test is shown in Figure 36.

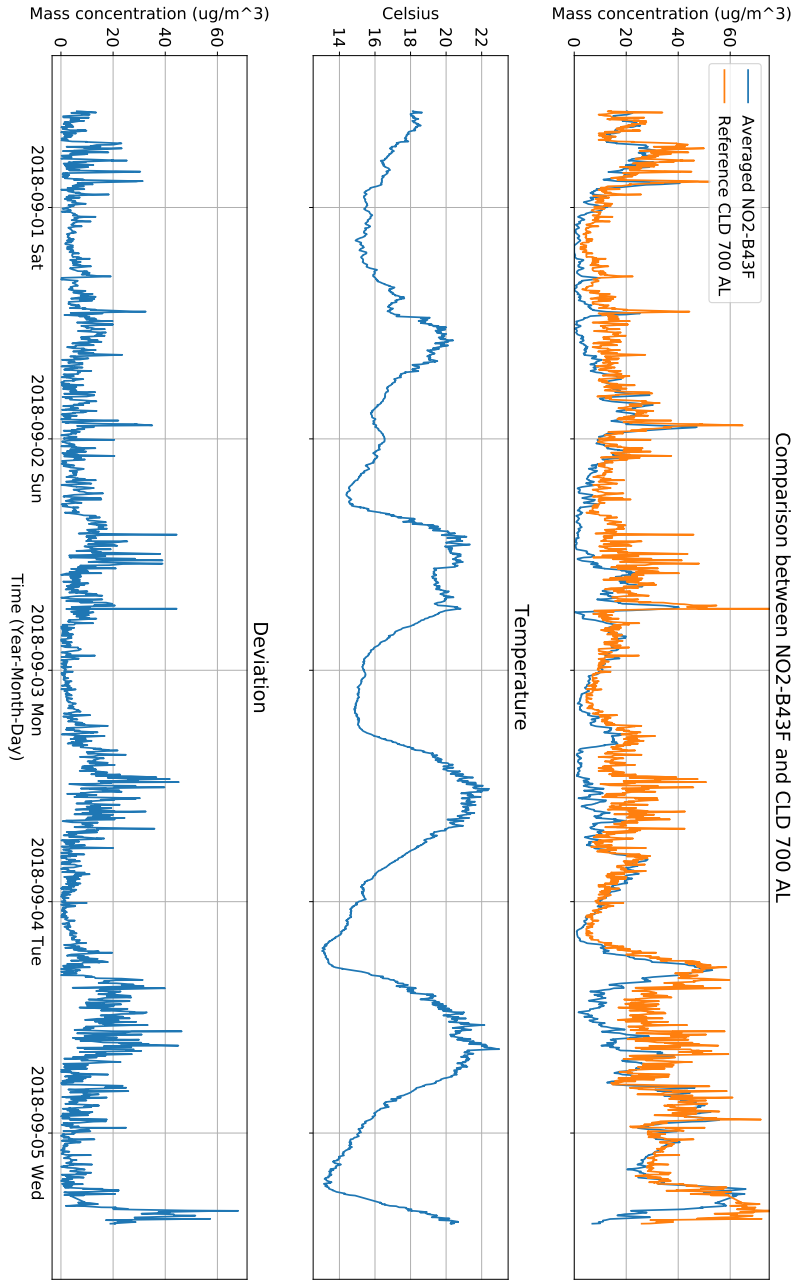

Figure 36: Results from the comparison with the CLD 700 AL chemiluminescence instrument. First plot shows mass concentrations for both units. Second plot shows the temperature measured by the measurement station. The third plot shows the difference between the NO_2 measurements of the NO2-B43F and reference.

Compared to the previous test the maximum deviation was higher, however, the measurements of the NO2-B43F have a more similar curve form to the reference than the first outdoor test in Lund, section 8.2.2. The levels of NO_2 measured by the NO2-B43F was generally lower than the reference, CLD 700 AL. The calculated statistics in Table 3 confirmed the observation. The Deming regression curve in Figure 37 indicates that the systematic error is significantly smaller compared to the first comparison, from the line it can be read that the NO2-B43 is making slightly lower measurements than the CLD 700 AL. It can also be seen that the error distribution is larger among the higher values and that the NO2-B43 does not capture all of the concentration peaks which is also shown in Figure 36. The R^2-value, 0.54, confirms the more similar curve shape. Figure 38, shows the NO2 measurements together with the surrounding O_3 levels, humidity and temperature. The weather data is measured by a weather station at Heleneholm which is located close to Dalaplan.

The Table 4, shows the daily averages of the session. Note that day 1 and 5 do not have a full day of averaging and therefore do not represent the true daily average of those days. Without the calibration, the deviations of day 2, 3 and 4 was above 5 µg/m^3. With the calibration, the deviation was below 3 µg/m^3, which shows that the calibration has a significant impact on the daily average calculation.

Table 3: Statistics of the error and bias between NO2-B43F and CLD 700 AL. The numbers are based on the data from the evaluation

NO2(Malmö)	Uncalibrated	Calibrated
Average absolute error	7.84 µg/m^3	6.1 µg/m^3
Standard deviation	7 µg/m^3	5.2 µg/m^3
Abs. error [Min, Max]	$[0, 44.3]$ µg/m^3	$[0, 32.8]$ µg/m^3
Bias	-30 %	0 %
R^2	0.54	

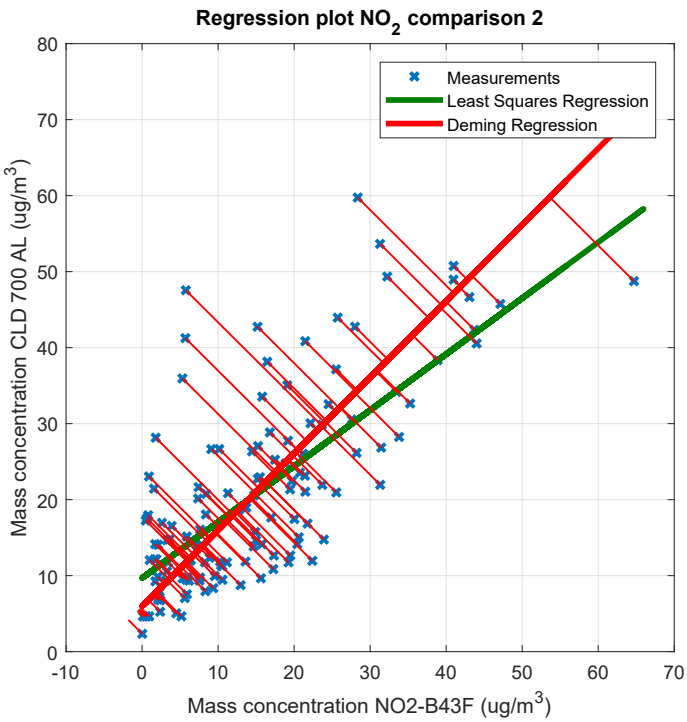

Figure 37: Plot showing estimated Deming and least square regression line with NO2-B43F on the x-axis and CLD 700 AL on the y-axis.

Daily avg.	Day 1 Sat	Day 2 Sun	Day 3 Mon	Day 4 Tue	Day 5 Wed
Uncal.	18.3	8.1	10.1	9.4	33.9
Cal.	23.9	15.9	17.5	17.0	35.9
CLD 700	21.7	13.4	16.6	16.1	41.8
Dev. uncal.	3.4	5.3	6.5	6.6	7.9
Dev. cal.	2.1	2.5	0.9	0.9	5.9

Table 4: The daily average of the measurements from Malmö. Only day 2, 3 and 4 have 24 hours of averaging. The calibrated values area calculated by applying the calibration factor from the linear regression. The values in this table are in µg/m^3.

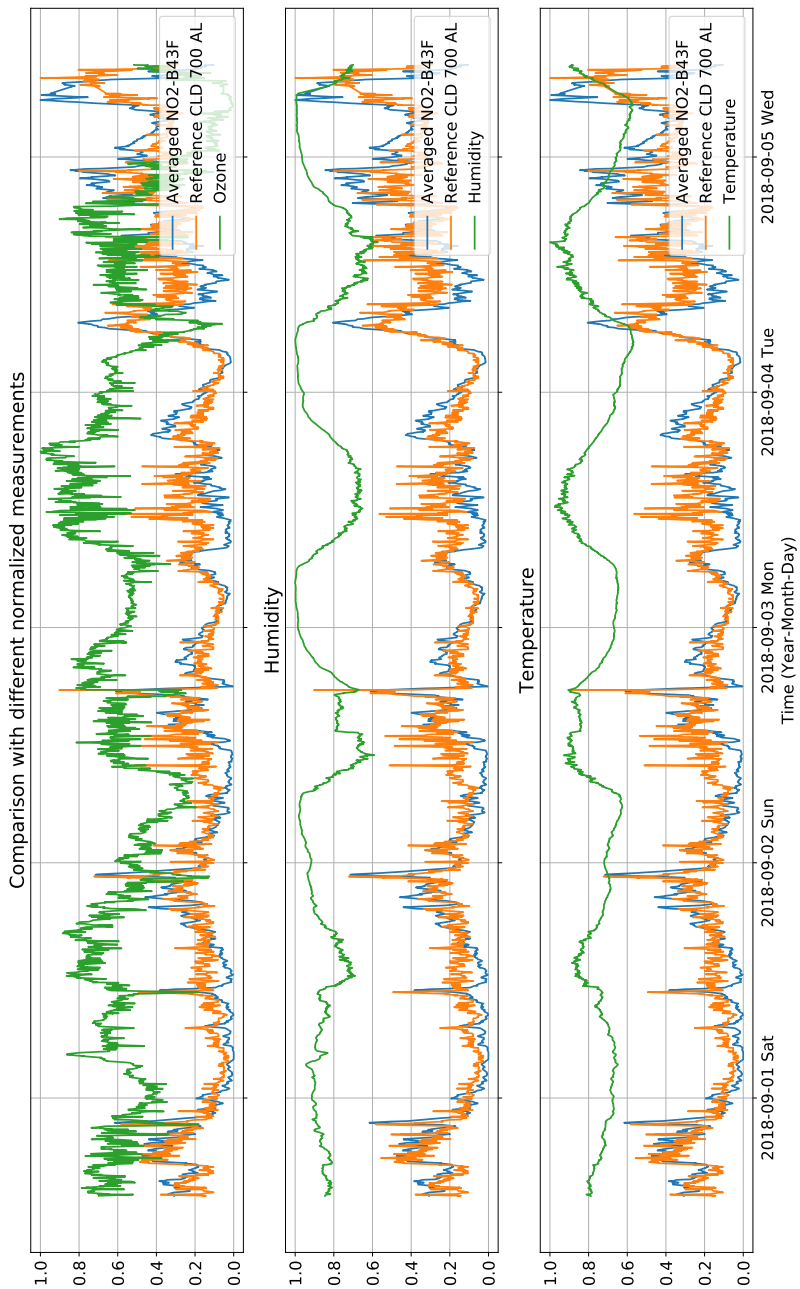

Figure 38: The subplots show different measurements compared with the NO2-B43F measurements. The measurements are normalised with itself to give a better plot for comparison.

The O_3 level was $[0.29, 83.94]$ µg/m^3, humidity level was $[54.26, 94.8]$ %, and the temperature level was $[13.02, 22.99]$ °C. The first comparison was with the O_3

level. The plot shows there was very little cross-sensitivity with the NO2-B43F sensor and O_3. When the O_3 level increased, no obvious correlations on the measurements of the NO2-B43F was observed. The following comparison was with humidity. While it was not obvious, every time the humidity went down, the measurements of the NO2-B43F went under the reference value. Likewise, when the humidity went up, the measurements of the NO2-B43F went above the reference value. The transients observed on the temperature climate test in Figure 32, cannot be observed on the measurements. The changes of temperature were not as fast as in the climate test, and therefore did not have an effect.

8.2.4 Particle matter and particle counter comparison with other OPCs

The measured mass concentration for the DustTrak and OPC-N2 sensor is shown in Figure 39 and 40. During the first session, the OPC-N2 makes a lower estimation than the DustTrak, but in the second half their values are very similar. Similarities in the curve shape can be observed during the whole session.

During the second measurement session the curve shape of the Alphasense is still similar, but it underestimates a bit and is not as responsive as the DustTrak during the peaks. A calibration factor with a first order polynomial was calculated using a curve fitting function in MATLAB, shown in Equation (7). With this applied, a more similar shape was achieved. The same calibration factor was used to compensate the first curve, resulting in a good curve fitting during the first half of the measurement period.

$$kx + m = 1.515x + 1.555 \tag{7}$$

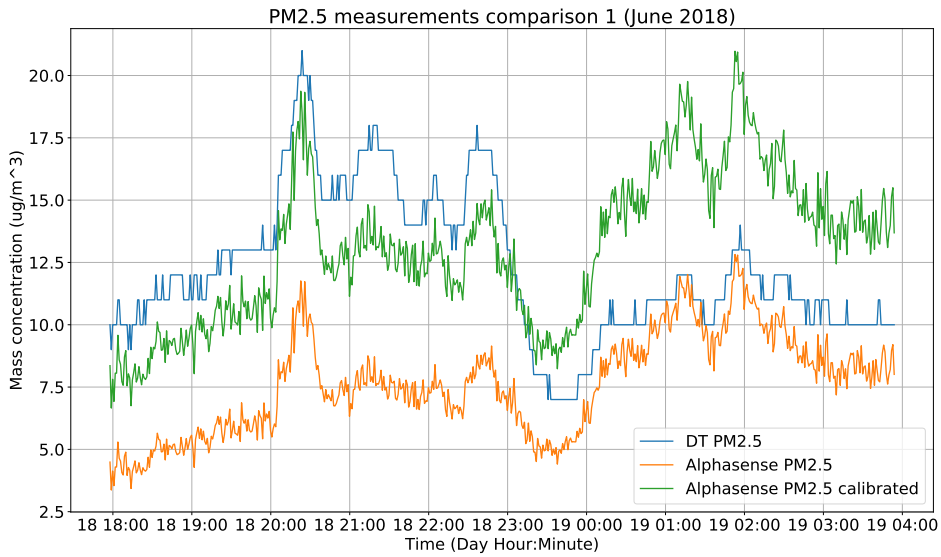

Figure 39: Plot shows the measurement data from the first measurement session. The comparison is between the DustTrak and Alphasense OPC-N2

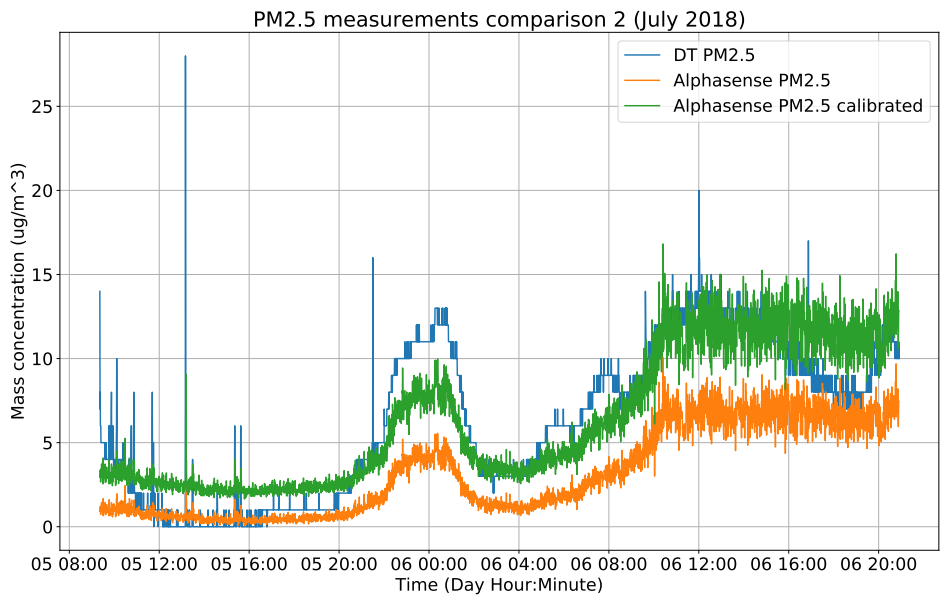

Figure 40: Plot shows the measurement data from the second measurement session at LTH. The OPC-N2 data is scaled with a kx+m polynomial to obtain a better fitting

Statistics from the second measurement session can be seen in Table 5. The

error data is based on the difference between the OPC-N2 and the DustTrak. The DustTrak is not a reference instrument which makes it difficult to make a statement about the reliability of the OPC-N2. In the regression plot in figure 41. It is clear that the OPC-N2 makes a lower estimation than the DustTrak. The error distribution is generally located close to the regression line. This is also reflected by the high R^2 coeffecient. The daily average of the second measurement session is shown in Table 6. Considering the daily limit of $PM_{2.5}$ is 25 $\mu g/m^3$, a deviation of 0.4 $\mu g/m^3$ is less than 10% of the limit. However, this was only from a single daily average and many more averages are needed to determine how accurate the sensor is in terms of daily averages.

Table 5: Statistics of the error and bias between OPC-N2 and the DustTrak. The numbers are based on the data from the second measurement session.

PM	Uncalibrated	Calibrated
Average absolute error	$3.3\,\mu g/m^3$	$1.7\,\mu g/m^3$
Standard deviation	$2.4\,\mu g/m^3$	$1.2\,\mu g/m^3$
Abs. error [Min, Max]	$[0, 27.5]\,\mu g/m^3$	$[0, 25.6]\,\mu g/m^3$
Bias	$50\,\%$	0%
R^2	0.773	

Daily avg.	Comparison 2
Uncal.	2.1
Cal.	4.8
DT 25	5.2
Dev. uncal.	3.1
Dev. cal.	0.4

Table 6: The daily average from comparison 2, Figure 40. The averaging was done from 12:00 to 12:00 in the next day. The values are in $\mu g/m^3$.

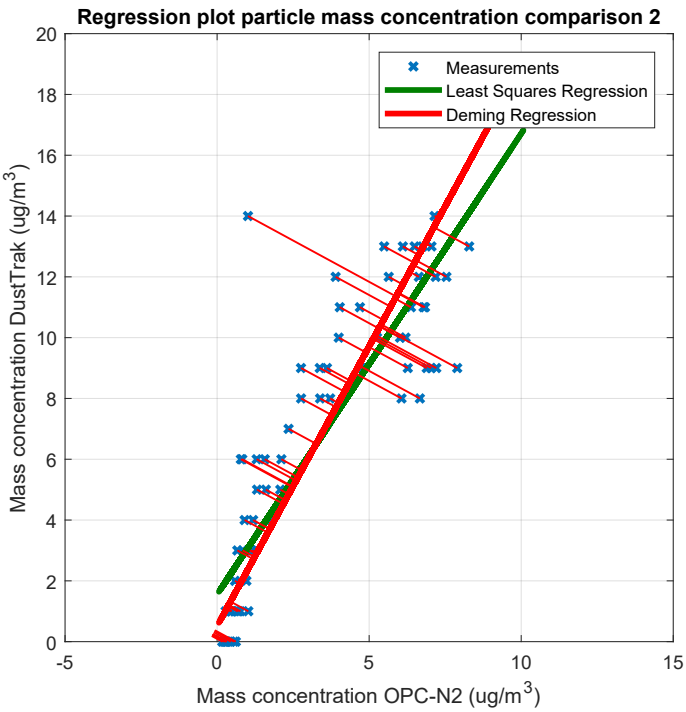

Figure 41: Plot showing estimated Deming and least square regression line with OPC-N2 on the x-axis and the DustTrak on the y-axis.

The results of the particle counting test can be obtained in Figure 42. The OPC-N2 underestimates particles in range between 0.5 and 0.7 µm. Another evaluation also concluded that the OPC-N2 underestimated in this size range [52]. In the size range between 0.7 and 3 µm they are more similar in their estimations. In the range between 1 and 3 µm the estimations are even better. In the last plot, which shows particle numbers in the range between 3 and 5 µm, the OPC-N2 gives an estimation with a lot of noise compared to the BioTrak. An important thing to consider is that the scale of the last plot is much smaller than the other plots, which magnifies the noise in comparison to the other plots.

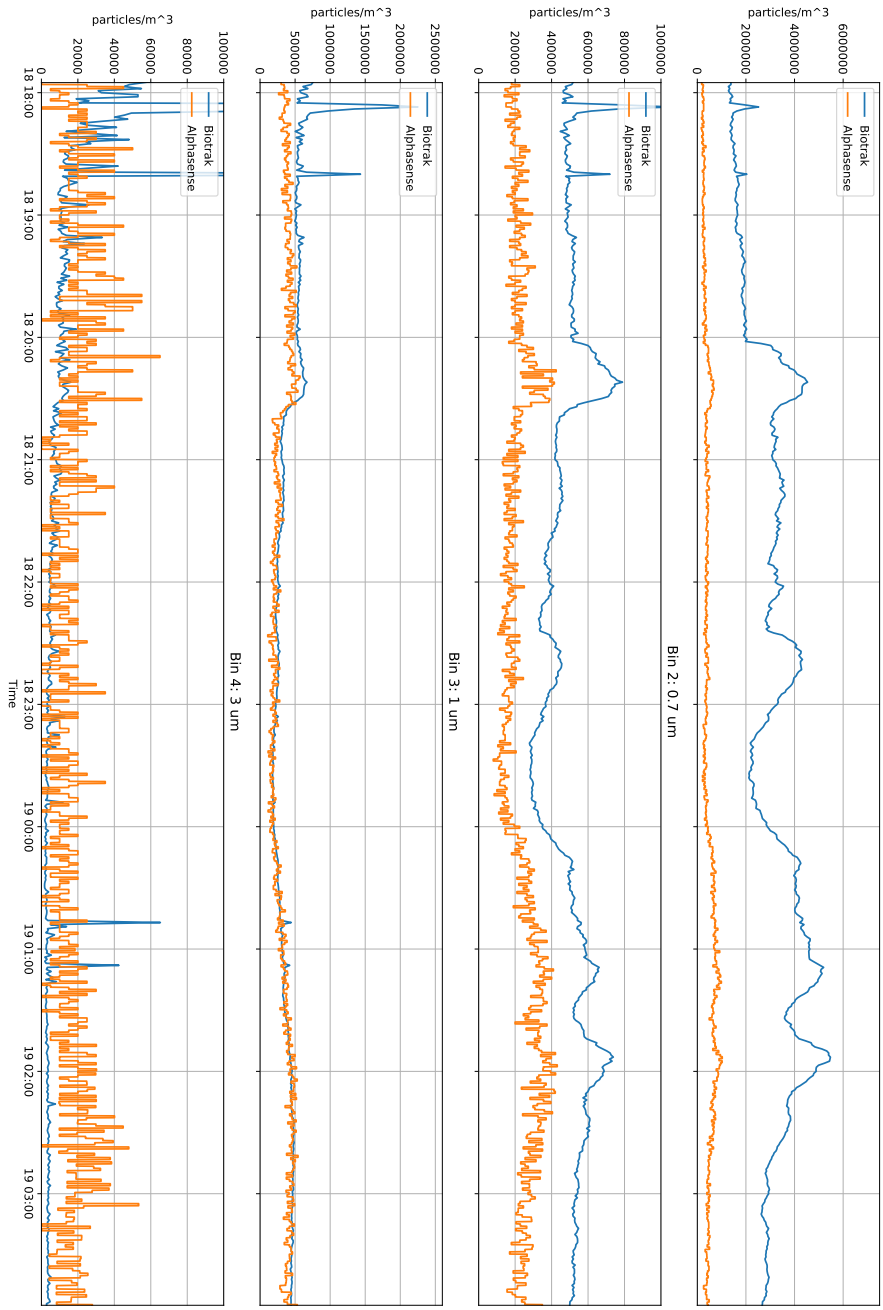

Figure 42: The comparison with the particle counter. First plot shows number of particles in the size range 0.5 to 0.7 µm. Second plot shows particles in the range 0.7 to 1 µm. Third plot shows particles in the size range 1 to 3 µm. Last plot shows particles between 3 and 5 µm.

9 Discussion and Conclusions

In the study from Balz Maag [20], there was a clear correlation between the sensor output and O_3 level, and measurement values of NO_2 where the O_3 level was higher than 3 ppb, 6 µg/m^3, was discarded. To reduce the impact of cross sensitivity, the Alphasense sensor has a built-in O_3 filter. In this study, no significant cross sensitivity was detected, even though the O_3 levels was as high as 41 ppb, 82 µg/m^3. A possibility is that Alphasense has reviewed and improved the sensor, although it still has the same model name. Rapid temperature and humidity proved to be a larger concern in this study, which was observed in both the field study and the controlled tests in the climate chamber.

A concern with the climate test, specifically the temperature test, was the mass concentration of NO_2. In an open system where gases can expand freely, the gas concentration varies depending on the temperature. According to the ideal gas law:

$$PV = nRT,$$

which P is pressure (N/m^2), V is volume (m^3), R is the ideal gas constant (8.31 J/(mol·K)), T is temperature (K) and n is a number of moles in a gas, an increase of temperature while keeping the pressure and volume constant will yield a lower moles of a gas. In section 8.2.1, with the results from the temperature test in Figure 32, a decrease in NO_2 level was observed with increasing temperature. In reality, the temperature has very little impact on the mass concentration and the decreasing NO_2 levels measured by the sensor is from the electrochemistry of the sensor reacting to the temperature changes [27].

In the last test of the NO_2, section 8.2.3, the humidity had visible effect on the sensor. Given how the sensor reacted in the humidity climate test, section 8.2.1, it was expected that the sensor would react to humidity in the outdoor evaluation as well. This was also observed in the first outdoor test, section 8.2.2, where the measurements increased above the reference while the temperature decreased, which implies the humidity also increased.

Given that the sensor was affected by the same factors in both of the outdoor tests. The dissimilarity of the R^2 in the first and last test suggested something was significantly different. In the case of the first test where a DOAS was used, the instrument measured over a distance. As for the CL instrument used in the last test, it measured in a point. The fact that the reference compared measures differently was a possible reason why R^2 dissimilar, and not because the final prototype made a difference to the measurements.

The function of the auxiliary electrode in the NO2-B43F was questioned in the study by Balz Maag [20]. There are two ways of calculating the NO_2 value from the sensor output. The one employed in this report was using the auxiliary electrode to subtract the offset voltage of the working electrode. The other one, considered to be the better solution by Balz Maag, was using the provided zero offset voltage from

Alphasense. The zero offset voltage is different for every sensor and in the case of the sensor used in the prototype the zero offset is labelled as WE zero in Table 1, with the value of 243 mV. The zero offset used in Balz Maag's study was 225 mV. The reasoning behind why the use of the auxiliary electrode was questionable, was because of the additional noise and no noticeable improvement over the use of the provided zero offset. It was however shown in the climate test of the prototype, that the auxiliary electrode reacted with the environmental changes. In every step change in temperature, Figure 32, the auxiliary voltage follows the transient of the working electrode. In the measured NO_2 level, this transient effect was minimised. If the provided zero offset was used instead, the transients would have a bigger effect on the measured NO_2 level. The same observation was made on the humidity test, Figure 33, with the slowly increasing auxiliary offset. The auxiliary electrode is certainly not perfect, but without the auxiliary electrode, the measured NO_2 values would have reacted more to the environmental variations. The noise of the auxiliary did not pose a big problem as the measurement was averaged and the ADC has its own filtering functionality activated.

9.1 The future of low-cost sensors

The low-cost sensors evaluated in this thesis show promising results. They are however not accurate enough to be used for regulatory measurements and it is a challenge to compensate for all of the weaknesses of these sensors. The main point, however was not to replace the reference instrument but used as a local complement to the reference. There are several future applications. In a place like Malmö, Dalaplan, the measurements from the measurement station, combined with other information, such as weather, is used for modelling to estimate local pollution. To replace modelling by installing low-cost sensors, the cost of the sensors has to be lower. It is estimated that the cost of modelling will be around 100 000 SEK [27], and with the current price at which the sensor units costs around 4 000 SEK, it is possible to replace modelling with real measurement data. The cost assumes that the place has all the necessary network infrastructure required to collect data from every sensor unit. In countries where air pollution is a big concern, projects with air sensor network have already started with funds from the government. A project in China, concerning air sensor networks, is ongoing. The air sensors are placed around the city. With the data points, a map is drawn over the city to visualise the pollution levels in different areas of the city. The data are also used to trace sources of pollution and are used as a proof to take further action in mitigating the polluted air [53].

The idea behind a smart city requires interconnected low-cost sensors. Assuming the city have installed network cameras all around the city, these small low-cost sensors that can connect directly to the camera for power and data communication is a future not too distant. The prototype for NO2-B43F developed in this thesis can be considered as a first step for such a concept.

An accessory box with many air sensors that is connected to a network camera is the most logical. This allows the customer to keep their current cameras in their installations and simply connect the accessory box to the I/O-port of the camera. An external box also allows flexibility in the placement of the box, so it can be placed closer to the area of interest. Modifications to the hardware will not be necessary. When the air sensors in the accessory box needs to be calibrated or replaced, it will be easy to disconnect the box.

The output of a low-cost sensor has many unknown correlations with factors beside the target quantity. This makes it hard to model and calibrate. With many sensors placed the random errors can be averaged out but the systematic errors cannot be averaged out. With computational power and reliable sets of statistical data, there is potential it may be possible to find the correlations and compensate for it. There are already sensor networks made up of low-cost sensors [54]. Reliable data set can also be found from the reference measurement stations placed around the country and with the advent of machine learning, this is certainly one of the most promising way to utilise low-cost sensors.

9.2 Future work

The tests performed shows the general behaviour of the sensor. It is however not a full study on how the sensor perform in all possible circumstances. To study deeper on the behaviour of the sensors, tests conducted on the sensors need a controlled environment with known air content. For the OPC-N2 it would be measuring air mixtures with known particle content, and for the NO2-B43F it would be air mixture with known gas content. To verify the air content, reference instruments need to be used. The humidity and temperature needs to be controlled as well to make sure these factors does not affect the sensor.

It may be possible to make a better calibration curves for the NO2-B43F. If the calibration curves were to be better it should at least calibrate for temperature and humidity as these have prominent effects on the NO2-B43F. It was planned to implement a combined temperature and humidity sensor in the final prototype to compensate for temperature and humidity, but because of the pins used in the SD-card library, the combined sensor was never implemented. If the effect of these parameters were to be studied one parameter should be varied while the others should be kept constant. In the case of calibration to compensate the humidity, the slope of humidity might be a better variable to use instead of the humidity level. From the results, it is the change of humidity that affected the sensor the most and not the level of humidity.

In a similar manner, the calibration curve for the OPC-N2 can be determined. The parameter worth considering is humidity. The refractive index of particles is affected by the amount of water in the air and as the estimation of particle mass is based on a fixed refractive index it could result in a faulty value. A study by

Leight R, Crilley, University of Birmingham,[55] have added a correction factor for humidity with great success. The calibration factor used in the evaluation was from a specific data set obtained in one test. To verify the calibration factor tests in other environments are needed. It is known that the electrochemical sensor reacts to environmental changes and the OPC-N2 can be affected by humidity. Climate test of the OPC-N2 is also valuable information.

One of the criteria in the EPA Air Sensor Guidebook is precision. To get a good estimation of the precision of the sensors the target quantity has to be constant during the measurements. In the case of NO2-B43F it can be hard to get an good estimation of the precision. Keeping the sensor in a closed box does not guarantee a constant NO_2, as NO_2 reacts to other gases in air. A NO_2 generator with free flow would be ideal to keep the NO_2 level constant. A way to maximise precision in the measurements is using multiple sensors in the same measurement area and average their values.

The OPC-N2 used to evaluate the performance of low-cost PM sensor consumes more power than the I/O-port of the camera can deliver. When the tests were conducted the OPC-R1 was not available. According to Alphasense, the performance of OPC-R1 should be similar to OPC-N2, but using considerable less power. It should be possible to power the OPC-R1 through the I/O-port. The form factor of OPC-R1 is also smaller.

One important aspect of these low-cost sensor is the long term performance. The tests performed in the thesis was not enough get an insight of the long term performance of the sensors. With the final prototype, which has a attached power cable, it would be possible to evaluate its performance in more than just a few weeks. With the OPC-N2, an enclosure similar to the final prototype should be built and then make a long term test besides a reference station. An interesting take on the construction around the NO2-B43F could be an intake manifold with a blower, similar to the construction in the study made by Alessandro Bigi [19]. The benefits of the manifold would be to shield the sensor from ambient conditions, such as wind speed, as it would affect the diffusion in the membrane of the sensor.

How much of an improvement the final prototype over the initial prototype is still unknown. The measurements taken with the final prototype are not significantly less noisy and tests in similar conditions are required to estimate the improvements in the final prototype. By analysing how much actual noise is in the measurements, a cheaper ADC could be chosen. This is significant if the design were to be mass produced.

A PCB schematic

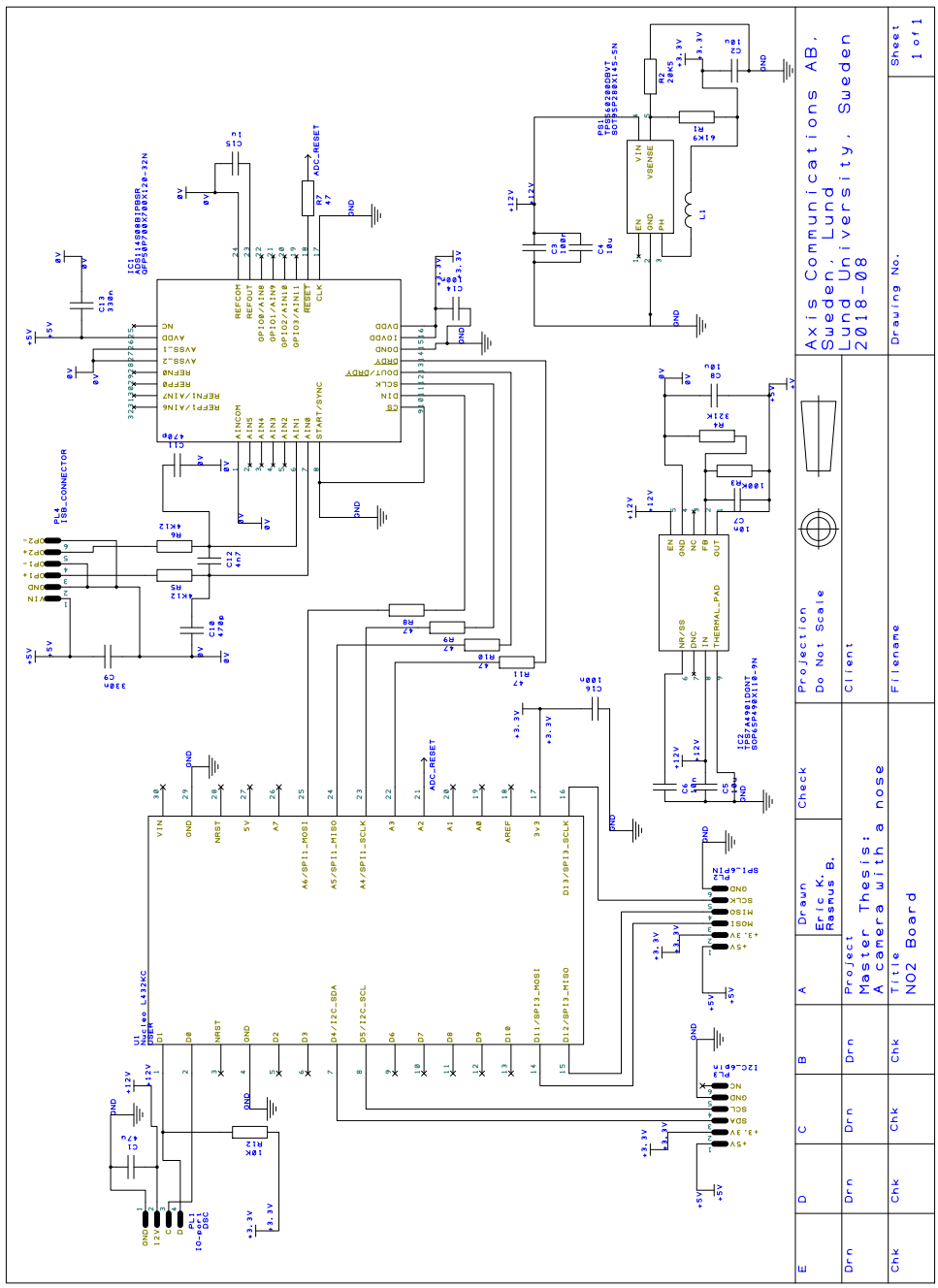

Figure 43: The schematics over the PCB.

B PCB layout

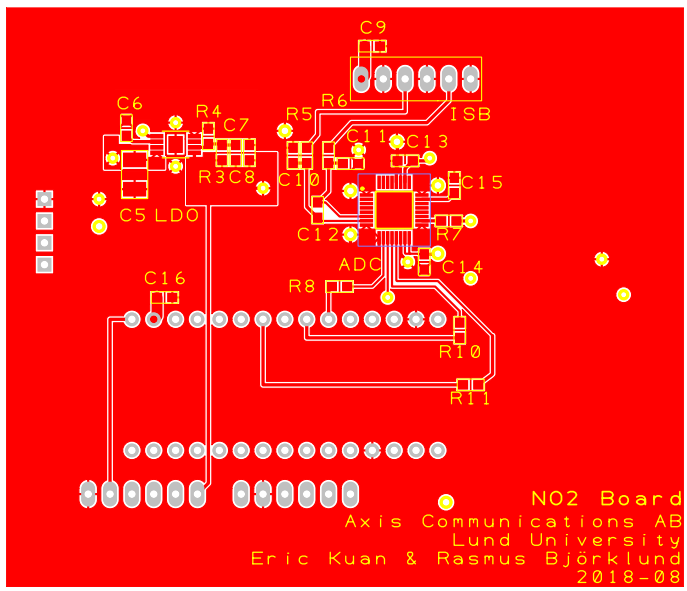

Figure 44: The top layer of the PCB. It is used as an analogue layer for noise sensitive components.

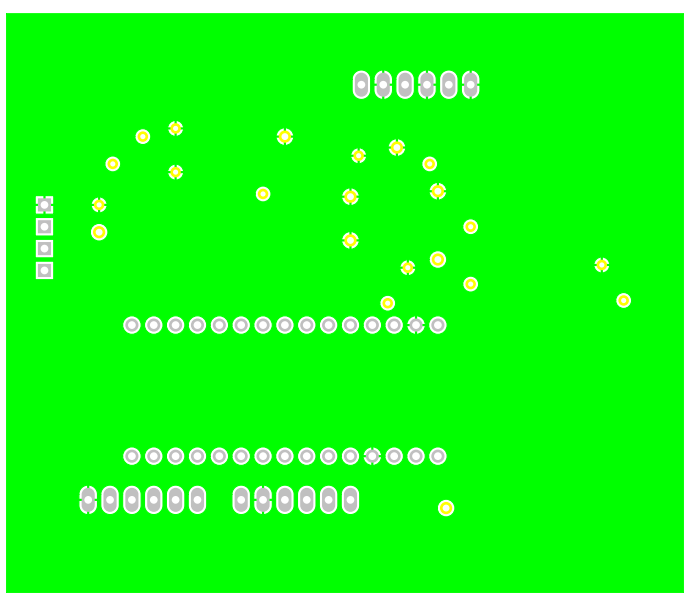

Figure 45: The second layer of the PCB and it is the ground plane.

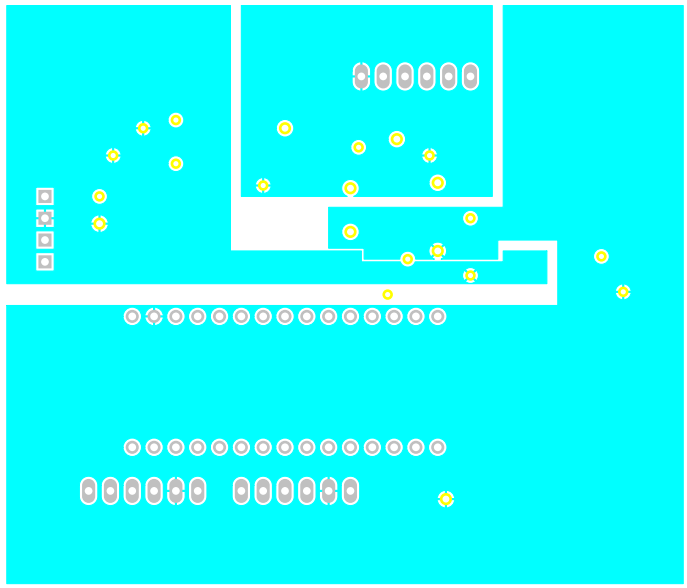

Figure 46: The third layer of the PCB. This layer is the power layer and is divided into three parts: 12 V, 5 V and 3.3 V.

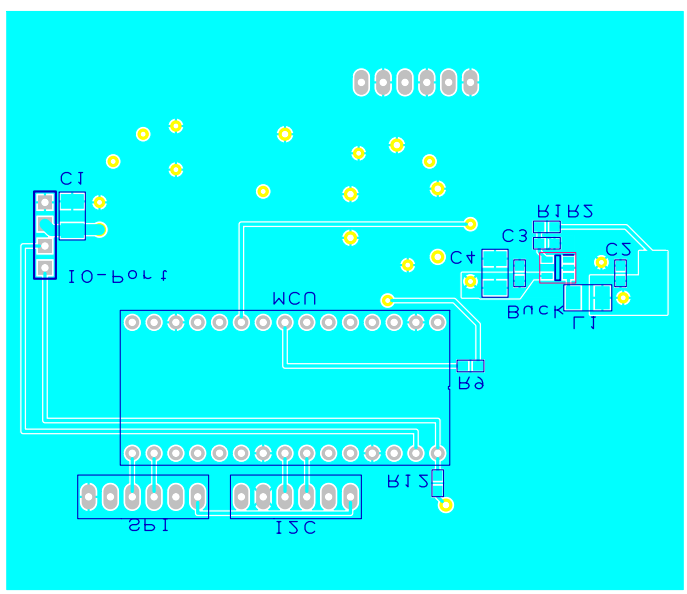

Figure 47: The bottom layer of the PCB consists of components that are less sensitive to noise.

References

[1] *Criteria Air Pollutants*. URL: https://www.epa.gov/criteria-air-pollutants (visited on 09/07/2018).

[2] *Godkända mätinstrument*. URL: http://www.aces.su.se/reflab/matningar/godkanda-matinstrument/ (visited on 03/07/2018).

[3] *MSHA's Occupational Illness and Injury Prevention Program Health Topic "Carbon Monoxide"*. URL: https://arlweb.msha.gov/illness_prevention/healthtopics/carbonmonoxide.htm (visited on 09/07/2018).

[4] Z. Yin et al. 'A Deep Normalization and Convolutional Neural Network for Image Smoke Detection'. In: *IEEE Access* (2017).

[5] *Split-Spectrum White Paper*. URL: https://nest.com/support/images/misc-assets/Split-Spectrum-Sensor-White-Paper.pdf (visited on 13/07/2018).

[6] *SBF 110:8 Regler för brandlarm*. Brandskyddsföreningen Sverige. 2017. URL: https://www.brandskyddsforeningen.se/webbshop/litteratur-och-produkter/sbf-1108/ (visited on 09/07/2018).

[7] Chaoyang Jiang et al. 'Indoor occupancy estimation from carbon dioxide concentration'. In: *Energy and Buildings* (14th Sept. 2016).

[8] Kevin Weekly et al. 'Low-cost coarse airborne particulate matter sensing for indoor occupancy detection'. In: *Building Efficiency and Sustainability in the Tropics (SinBerBEST)* (17th Aug. 2013).

[9] *the semiconductor gas sensing technique*. URL: https://www.edaphic.com.au/gas-detection-encyclopedia/semiconductor-sensors/ (visited on 26/08/2018).

[10] Philip J. D. Peterson et al. 'Practical Use of Metal Oxide Semiconductor Gas Sensors for Measuring Nitrogen Dioxide and Ozone in Urban Environments'. In: *MDPI sensors* (19th July 2017).

[11] *Lecture 5 : Instrumentation techniques to monitor SO2 pollution*. URL: https://nptel.ac.in/courses/104103020/module3/lec5/6.html (visited on 26/08/2018).

[12] *Absorption spectroscopy*. URL: https://en.wikipedia.org/wiki/Absorption_spectroscopy#/media/File:Spectroscopy_overview.svg (visited on 27/08/2018).

[13] *Luftkvalitetsmätningar i Lunds kommun för år 2016 samt luftmätningsdata för åren 1990 – 2016*. https://www.lund.se/globalassets/lund.se/bygg_bo/buller-och-luftkvalitet/luften-utomhus/rapporter-luftmatningar/2016/luften-i-lund-2016-med-jamforande-matningar-1990-2016.pdf. 2017.

[14] Marwa M. Ragheb Mazen Erfan Yasser M. Sabry and Diaa A. Khalil. *Optical Gas Sensing with MEMS FTIR Spectrometers*. Washington: SPIE Press, 2017. ISBN: 9781510613690.

[15] *CLD Principles*. URL: https://www.cambustion.com/products/cld500/cld-principles (visited on 27/08/2018).

[16] Jörg Kleffmann et al. 'NO_2 Measurement Techniques: Pitfalls and New Developments'. In: *Disposal of Dangerous Chemicals in Urban Areas and Mega Cities*. 2013.

[17] Judith Graham. *Nitrogen oxides*. http://www.inchem.org/documents/ehc/ehc/ehc188.htm. Geneva: World Health Organization, 1997. ISBN: 9241571888.

[18] David Joseph and Amit Kumar. 'Static Laser Light Scattering Studies from Red Blood Cells'. In: 06 (Jan. 2016), pp. 237–260.

[19] Alessandro Bigi et al. 'Performance of NO, NO_2 low cost sensors and three calibration approaches within a real world application'. In: *Atmospheric Measurement Techniques* (26th June 2018).

[20] Balz Maag. 'Sense The Air You Breathe!' Semester Thesis. Switzerland, ETH Zürich Department of Information Technology and Electrical Engineering, 20th Dec. 2013.

[21] *Health and Environmental Effects of Particulate Matter (PM)*. URL: https://www.epa.gov/pm-pollution/health-and-environmental-effects-particulate-matter-pm (visited on 27/08/2018).

[22] Ron Williams et al. *Air Sensor Guidebook*. Report EPA 600/R-14/159. Washington, DC: U.S. Envrionmental Protection Agency, 2014.

[23] *Preciseringar av Frisk Luft*. URL: http://www.sverigesmiljomal.se/miljomalen/frisk-luft/preciseringar-av-frisk-luft/ (visited on 11/07/2018).

[24] *Kvävedioxid i luft*. URL: https://www.miljomal.se/Miljomalen/Alla-indikatorer/Indikatorsida/?iid=90&pl=1 (visited on 29/06/2018).

[25] *Luften i Malmö 2017*. Malmö stad miljöförvaltningen. Apr. 2014. URL: https://malmo.se/download/18.270ce2fa16316b5786c215a/1525439220055/Rapport_nr_4_Luften_i_Malmo2017.pdf (visited on 29/06/2018).

[26] *Air quality standards*. URL: https://www.eea.europa.eu/themes/air/air-quality-standards (visited on 29/06/2018).

[27] Mårten Spanne. personal communication. 23rd Aug. 2018.

[28] *Application Note AAN104: How Electrochemical Gas Sensors Work*. Alphasense. 2018.

[29] *Alphasense Application Note AAN 110: Environmental changes: Temperature, Pressure, Humidity*. Alphasense. 2018.

[30] *hazardex: Understanding gas sensor lifespan*. URL: http://www.hazardexonthenet.net/article/128977/Understanding-gas-sensor-lifespan.aspx (visited on 22/09/2018).

[31] *Particle pollution*. URL: https://airnow.gov/index.cfm?action=aqibasics.particle (visited on 29/06/2018).

[32] Naturvårdsverket. *Naturvårdsverkets föreskrifter om kontroll av luftkvalitet; NFS 2016:9*. https://www.naturvardsverket.se/Documents/foreskrifter/nfs2016/nfs-2016-9.pdf. 2016.

[33] *Harmonisering QA/QC*. Referenslaboratoriet för tätortsluft. 5th Mar. 2018. URL: http://www.aces.su.se/reflab/wp-content/uploads/Harmonisering-QAQC.pdf (visited on 03/07/2018).

[34] *Optical particle Counters*. URL: http://www.cas.manchester.ac.uk/restools/instruments/aerosol/opc/ (visited on 04/07/2018).

[35] *Datasheet NO2-B43F*. Alphasense. 2016. URL: http://www.alphasense.com/WEB1213/wp-content/uploads/2017/07/NO2B43F.pdf.

[36] *Datasheet 3SP_NO2_5F P Package 110-507*. SPEC Sensors. 2017. URL: https://www.spec-sensors.com/wp-content/uploads/2016/10/3SP_NO2_5F-P-Package-110-507.pdf.

[37] *De-construction of the Shinyei PPD42NS dust sensor.* URL: http://takingspace.org/wp-content/uploads/ShinyeiPPD42NS_Deconstruction_TracyAllen.pdf (visited on 12/07/2018).

[38] Bernd Laquai. ‘Impact of Particle Mass Distribution on the Measurement Accuracy of Low-Cost PM-Sensors’. In: (Oct. 2017). URL: https://www.researchgate.net/publication/320537200_Impact_of_Particle_Mass_Distribution_on_the_Measurement_Accuracy_of_Low-Cost_PM-Sensors.

[39] *Datasheet OPC-R1*. Alphasense. 2018. URL: http://www.alphasense.com/WEB1213/wp-content/uploads/2018/02/OPC-R1.pdf.

[40] *STM32L432KB STM32L432KC*. STMicroelectronics. 2018. URL: https://www.st.com/resource/en/datasheet/stm32l432kc.pdf.

[41] *Datasheet ATmega328/P*. Atmel. 2016. URL: http://ww1.microchip.com/downloads/en/DeviceDoc/Atmel-42735-8-bit-AVR-Microcontroller-ATmega328-328P_Datasheet.pdf.

[42] Paul Henry Kaye and Edwin Hirst. ‘Second Generation Low-Cost Particle Counter’. US20130229655A1. 5th Sept. 2013.

[43] *Alphasense User Manual OPC-N2 Optical Particle Counter*. Alphasense Limited. Dec. 2015.

[44] *Alphasense 4-Electrode Individual Sensor Board (ISB) User Manual*. Alphasense Limited. May 2017.

[45] *ADS114S0x Low-Power, Low-Noise, Highly Integrated, 6- and 12-Channel, 4-kSPS, 16-bit, Delta-Sigma ADC with PGA and Voltage Reference*. Texas Instruments. June 2017.

[46] *TPS7A49 36-V, 150-mA, Ultralow-Noise, Positive Linear Regulator*. Texas Instruments. May 2015.

[47] *TPS560200 4.5-V to 17-V Input, 500-mA Synchronous Step-Down Converter With Advanced Eco-Mode™*. Texas Instruments. Sept. 2013.

[48] *TPS7A30-49EVM-567 User’s Guide*. Texas Instruments. Aug. 2010.

[49] *Evaluation Module for TPS54061 Synchronous Step-Down SWIFT*. Texas Instruments. May 2012.

[50] *Diecast Boxes: Metal enclosure grey 112 x 62 x 31 Die cast aluminium*. RND components.

[51] dhhagan. *opcn2*. https://github.com/dhhagan/opcn2. 2018.

[52] Sinan Sousan et al. ‘Evaluation of the Alphasense optical particle counter (OPC-N2) and the Grimm portable aerosol spectrometer (PAS-1.108).’ In: *Aerosol Science & Technology* 50.12 (2016), pp. 1352–1365. ISSN: 02786826. URL: http://ludwig.lub.lu.se/login?url=http://search.ebscohost.com/login.aspx?direct=true&db=a9h&AN=119615805&site=eds-live&scope=site.

[53] *Fairsense*. URL: http://www.fairsense.cn/index.htm (visited on 11/09/2018).

[54] *Luftdata*. URL: https://luftdata.se/ (visited on 29/08/2018).

[55] Crilley L. R. et al. 'Evaluation of a low-cost optical particle counter (Alphasense OPC-N2) for ambient air monitoring.' In: *Atmospheric Measurement Techniques, Vol 11, Pp 709-720 (2018)* (2018), p. 709. ISSN: 1867-1381. URL: http://ludwig.lub.lu.se/login?url=http://search.ebscohost.com/login.aspx?direct=true&db=edsdoj&AN=edsdoj.6bd941d69e7f4aea93594061bebc8da7&site=eds-live&scope=site.